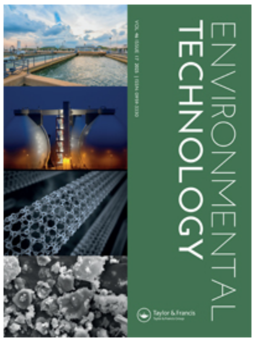

Taylor & Francis
Taylor & Francis Group

Environmental Technology

ISSN: 0959-3330 (Print) 1479-487X (Online) Journal homepage: www.tandfonline.com/journals/tent20

Influence of support medium height on the optimization of performance of an Upflow Anaerobic Hybrid Reactor (UAHB) treating synthetic wastewater

Alvaro Javier Esteban Villota Mora, Yeimy Ordoñez Muñoz, Eduardo Borges Lied, Vsevolod Mymrin, Karina Querne de Carvalho & Fernando Hermes Passig

ENVIRONMENTAL TECHNOLOGY
https://doi.org/10.1080/09593330.2025.2519960

Influence of support medium height on the optimization of performance of an Upflow Anaerobic Hybrid Reactor (UAHB) treating synthetic wastewater

Alvaro Javier Esteban Villota Mora [a], Yeimy Ordoñez Muñoz [a], Eduardo Borges Lied [b], Vsevolod Mymrin [a], Karina Querne de Carvalho [c] and Fernando Hermes Passig [d]

[a]Civil Engineering Graduate Program, Federal University of Technology – Paraná (UTFPR), Curitiba, Brazil; [b]Department of Biological and Environmental Sciences, Federal University of Technology – Paraná (UTFPR), Medianeira, Brazil; [c]Civil Construction Academic Department, Federal University of Technology – Paraná (UTFPR), Curitiba, Brazil; [d]Chemistry and Biology Academic Department, Federal University of Technology – Paraná (UTFPR), Curitiba, Brazil

ABSTRACT

The support media of upflow anaerobic hybrid reactors (UAHB) facilitates the formation and retention of microbial biofilm and the contact between the influent and microorganisms. Previous studies demonstrated the importance of support media height (SMH) to organic matter removal; however, the influence of this parameter in the UAHB reactor performance under varying conditions is still a gap. The Central Composite Design (CCD) method was applied to optimize the removal of organic matter by varying the cross-sectional area and height of the reactor based on 42 studies. The modelling indicated 72–87% COD removal efficiencies with 0.007 m^2 cross-sectional area and 0.75 m height, with 5.5 L total volume. Thus, three pilot-scale UAHB reactors, filled with Corrugated Polyvinyl Chloride (PVC) rings at different heights (6, 15, and 24 cm), were operated with a hydraulic retention time of 10 h, treating synthetic effluent with a COD of 490 $mgO_2\ L^{-1}$. Unlike previous studies, this study evaluated identical UAHBs operating in parallel under controlled conditions. The UAHB reactors presented stability, buffering capacity, and neutral pH during the operation. The reactor with higher SMH (24 cm) achieved higher removal efficiencies of turbidity (90%), COD (72.6%), and TS (63%). Variations in SMH affected reactor performance, as corroborated by the negative and 'very strong' correlation for turbidity, COD, and TS and a 'moderate' correlation for fixed and volatile solids. The novelty of this study lies in its comprehensive assessment of how varying SMH affects UAHB reactor performance, guiding future advancements in its design for efficient wastewater treatment.

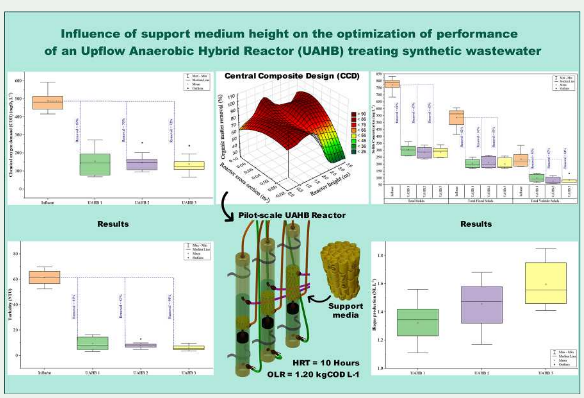

ARTICLE HISTORY
Received 13 November 2024
Accepted 30 May 2025

KEYWORDS
Anaerobic digestion; Central Composite Design (CCD) method; statistical planning; inert support medium; COD removal

1. Introduction

The upflow anaerobic hybrid reactor (UAHB) is a high-rate reactor that combines the benefits of the biological process of suspended growth by inserting an anaerobic filter inside the reactor to treat sanitary sewage and industrial wastewater [1]. This filter acts as a support medium, facilitates the formation and retention of microbial biofilm [2], distributes the flow uniformly, and allows solid–gas separation, thus improving the contact between the influent and microorganisms.

CONTACT Karina Querne de Carvalho kaquerne@utfpr.edu.br Civil Construction Academic Department, Federal University of Technology – Paraná (UTFPR), Deputado Heitor de Alencar Furtado St., 5000, Ecoville, 81280-340, Curitiba, Paraná, Brazil
Supplemental data for this article can be accessed online at https://doi.org/10.1080/09593330.2025.2519960.

Therefore, UAHB reactors can retain large amounts of biomass, reaching high removal efficiencies [3].

The biomass retained in the filtering material forms a biologically active structure known as biofilm, which acts as a physical barrier, preventing the solids from being washed out from the treatment system. Likewise, the microorganisms that cannot remain in the biofilm form a type of interstitial flocculant or granular sludge in the interstices [4]. Thus, the biomass retained inside the reactor appears as a layer of biofilm adhered to the support material surface, dispersed, removed from the cracks of the support material, or in the false bottom of the filtering material, released in the form of flakes or granules [5].

The surface of the support medium influences the treatment capacity of the UAHB reactors, facilitating the retention of the microbial population [6]. Changes in the microbial community structure can cause instability and a subsequent decline in the performance of these systems [5].

When in contact with the biomass, the organic compounds in the effluent are diffused through the biofilm surface or the granular sludge and converted into intermediate and final products, specifically methane and carbon dioxide [5].

Considering the influence of biofilm and support media in the performance of the hybrid reactors, further studies are still necessary to establish the optimal characteristics of the support medium under different operating conditions of the UAHB reactor.

Previous studies have examined different effluent sources, such as synthetic wastewater [7–10], domestic wastewater [3,11,12] effluents from slaughterhouses [13–15], agro-industrial activities [16–18], and other specific sources, such as coffee processing [19,20], distilleries [21,22], and pulp and paper manufacturing [23,24]. Despite differences in composition, COD removal efficiencies have generally been high, ranging between 60% and 99%, highlighting the effectiveness of the UAHB reactor operated under different conditions.

The selection of support media is fundamental to the treatment efficiency. Studies have used synthetic materials such as corrugated PVC rings [7,9,10], various forms of polypropylene structures [1,13,25], bio-balls [26,27], and natural materials like coconut shells and bamboo [3,28]. In general, synthetic media offer better stability and biomass retention, while natural materials, although more affordable and sustainable, may degrade or compact over time.

Another important factor is the height of the support media, which varies widely across studies, from less than 0.1 m [15] to over 1.0 m [29]. A greater support media volume typically enhances biomass retention and COD removal efficiency but can also lead to increased head loss and hydraulic flow disruptions within the reactor [30,31].

Da Silva Ramos et al. [7] achieved 90% organic matter removal (in terms of COD) and biogas production of 0.006 m^3 day^{-1} by using corrugated PVC rings in a UAHB reactor with a height of 1.0 m and a volume of 0.022 m^3. Similarly, Elmitwalli et al. [29] obtained 64% organic matter removal by applying reticulated polyurethane foam (RPF) type TM30 as a support medium (1.0 m of height) in a UAHB reactor with a height of 2.3 m, diameter of 0.19 m, and a volume of 0.07 m^3.

In addition, lower heights of the support media have also proven effective, as observed by Michelon et al. [9] and Godinho et al. [10], who used corrugated PVC rings forming a support medium with a height of 0.32 m, achieving organic matter removal (COD) of 85.4% and 81%, respectively. By using hose pieces as a support medium with a height of 0.6 m, Buyukkamaci and Filibeli [8] achieved 86% organic matter removal, reinforcing that selecting the appropriate material and support height is crucial for optimizing treatment. Similarly, Das and Chaudhari [12] observed positive results using sponge cubes with a height of 0.4 m, achieving 65% organic matter removal in a 2.7 m reactor.

Other applications with emergent materials have been successfully investigated for support media in anaerobic reactors with organic matter removal varying from 62% to 96%, such as polypropylene hexagons (specific surface area 6,700 m^2 m^{-3}) [13], coconut fibre polyvinyl (specific surface area 15,500 m^2 m^{-3}) and alcohol gel beads seashells (specific surface area 2,500 m^2 m^{-3}) [3], bamboo pieces (specific surface area approximately 415 m^2 m^{-3}) [28], a mix of ceramic, polypropylene, and rock (specific surface area approximately 92.09 m^2 m^{-3}) [18], among others.

The specific surface area of these materials varies considerably, with values ranging from 2,500 to 15,500 m^2 m^{-3}, depending on porosity and structural characteristics. A higher specific surface area promotes greater microbial attachment and biofilm formation, enhancing substrate degradation and biogas production [32]. Studies suggest that variations in both the height of the support medium and the material type significantly improve the reactor performance, increasing the organic matter removal [33,34].

Although there are different reactor configurations, most studies report high COD removal efficiencies, confirming the versatility and effectiveness of this technology in treating different types of effluents. Thus, the height of the support medium, material selection, porosity, and the dynamics of microbial colonization influence the reactor performance. Regarding optimizing the reactor performance, the ideal support medium height remains an open question since different effluents may require different reactor and support medium configurations, even with the knowledge that higher support medium heights favour biomass retention and treatment efficiency for some effluents.

Despite these promising results, there is still no consensus on the ideal combination of height, material type, and reactor configuration for different wastewater compositions. Furthermore, most studies have focused on organic matter removal, while long-term reactor stability remains underexplored. Another challenge is the lack of standardized methodologies for evaluating retention efficiency in different support media, making comparing results across studies difficult.

Thus, to address these gaps, we designed, operated, and evaluated the performance of three pilot-scale UAHB reactors with different heights of the support medium in treating synthetic wastewater, correlating the design, size, and height of the support medium with the organic matter removal efficiency. The innovative and original aspects of our study are based on the hypothesis that increasing the height of the support medium improves biomass retention and organic matter removal efficiency, optimizing the operation of the UAHB reactor. Besides that, unlike previous studies, this study evaluates the impact of support medium height on identical reactors operated in parallel and simultaneously under controlled conditions, allowing for a more precise comparison of the effect of this parameter on reactor efficiency. Thus, the external factors of room temperature, humidity, and feeding conditions did not influence the monitoring measurements since the reactors were installed at the exact location and fed simultaneously with the same influent.

The results of this study have direct implications for the design and operation of UAHB reactors, focusing on the optimization of the support medium configuration to maximize the treatment efficiency, reducing costs, and contributing to more sustainable treatment processes for industrial and domestic wastewater, aligned with the Sustainable Development Goals (SDGs).

2. Materials and methods

2.1. Analysis of preliminary studies for sizing the UAHB reactors

Figure 1 shows the methodological process flowchart developed in this study.

Based on the literature review regarding advances in upflow anaerobic hybrid (UAHB) reactors treating sanitary sewage (Table S1, Supplementary material), some of the most relevant sizing parameters (height, cross-section area, volume, and support medium height) were graphically correlated to the organic matter removal efficiency (in terms of COD).

The data collected in preliminary studies were organized and filtered for each selected sizing parameter. Subsequently, surface graphs were developed relating these sizing parameters of the treatment systems and the treatment performances regarding the organic matter removal. Two developed graphs allowed the selection of dimensions and thicknesses of the support medium for further applications in this study.

The first graph is related to the reactor cross-section, height, and organic matter removal efficiency (COD). In the second graph, the variables reactor volume and volume of support material inside the reactor were related to the variable removal of organic matter in terms of COD.

The results of the development of the analysis of the preliminary studies were considered for the design of the pilot-scale UAHB reactor and the operational parameters for this study.

2.2. UAHB reactors

The system, which consisted of three pilot-scale UAHB reactors, was arranged in parallel at the same height (Figure 2). The cylindrical reactors were built with identical volume and geometry in polyvinyl chloride (PVC) with 0.1 m of diameter (0.03 m thickness) and 1.0 m of height (each), resulting in a total volume of 5.5 L (each). The details of the reactor sizing are provided in Table 1, and the characteristics of the support media are referenced in the supplementary material (Table S2).

Each reactor was fed synthetic wastewater pumped from a PVC reservoir (128 L) by solenoid diaphragm metering pumps (ProMinent, model Concept plus) with a maximum flow rate of 8 L h^{-1} to promote equitative distribution. The reservoir stored the synthetic wastewater to guarantee the daily volume of effluent for the UAHB reactor feeding.

The UAHB reactors have identical characteristics, except for the sizing of the support media and, consequently, the characteristics depending on this parameter (Table S2, Supplementary material).

The hydrodynamic and mass transfer characteristics of the UAHB reactors were analyzed using dimensionless numbers and pressure drop calculations. The reactors 1, 2, and 3, with a diameter of 0.10 m and a useful height of 0.75 m, were operated under a continuous flow regime at flow rates of 0.55, 0.54, and 0.53 L h^{-1}, respectively.

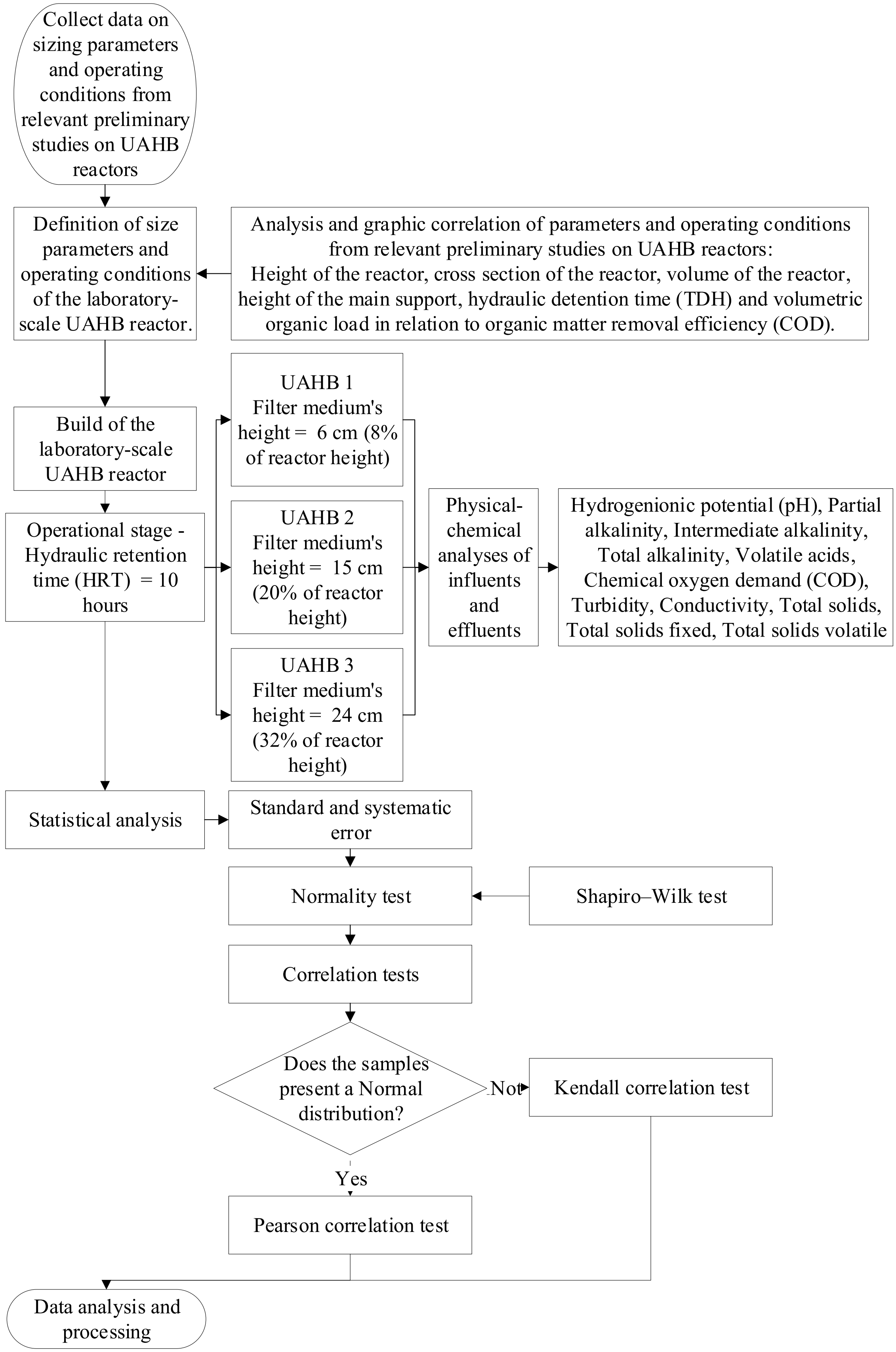

Figure 1. Flowchart of the methodological process.

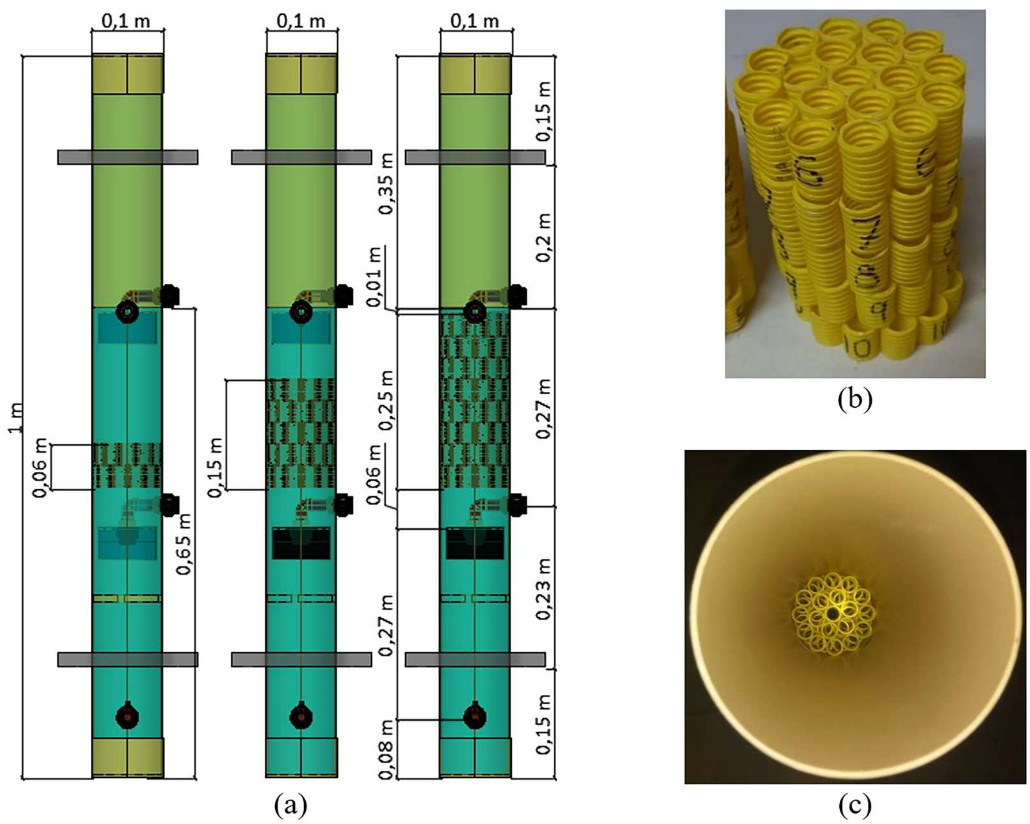

Figure 2. Scheme of the pilot-scale UAHB reactors (a); support media (b); inside the reactor (c).

The Reynolds number (Re) [35] was calculated to determine the flow regime within the reactor (Eq. 1).

$$Re = \frac{\rho v L}{\mu} \quad (1)$$

Table 1. Details of sizing of the UAHB reactors and support media

Parameter	UAHB 1	UAHB 2	UAHB 3
Sizing			
Cross-sectional area (m^2)	0.007	0.007	0.007
Water level height (m)	0.75	0.75	0.75
Support medium height (m)	0.06	0.15	0.24
Media configuration	38 rings (2 layers of 19 rings)	95 rings (5 layers of 19 rings)	152 rings (8 layers of 19 rings)
Installation height of the half support media from the bottom (cm)	40	40	40
% Support media height	8	20	32
Support media volume (L)	0.04	0.12	0.18
Support mediamass (g)	54.76	137.32	221.75
Support media surface area (cm^2)	3.236	7.069	11.757
Useful volume (L)	5.46	5.38	5.31
Design parameters and operational conditions			
HRT (h)	10	10	10
COD (mgO_2 L^{-1})	500	500	500
OLR (kgCOD m^{-3} d^{-1})	1.20	1.20	1.20
Q (L h^{-1})	0.55	0.54	0.53
V_{up} (m h^{-1})	0.079	0.077	0.076
V (L)	13.20	12.96	12.72

Note: HRT = Hydraulic Retention Time; Q = Influent flow rate; COD = Chemical oxygen demand; OLR = Organic Loading rate; V_{up} = upflow velocity; V = Volume of synthetic effluent prepared per day.

Where ρ is the density of water (998 kg m^{-3}), v is the average flow velocity (m s^{-1}), L is the characteristic length (m), and μ is the dynamic viscosity of water (1.002×10^{-3} Pa·s).

The Schmidt number (Sc) [36] (Eq. 2) and the Sherwood number (Sh) [37] (Eq. 3) were determined to evaluate the mass transfer efficiency. The Schmidt number relates momentum and mass diffusivity.

$$Sc = \frac{\mu}{\rho D} \quad (2)$$

Where D is the diffusivity of methane in water (1.3×10^{-9} m^2 s^{-1}), ρ is the density of water (998 kg m^{-3}), v is the average flow velocity (m s^{-1}), L is the characteristic length (m), and μ is the dynamic viscosity of water (1.002×10^{-3} Pa·s).

The Sherwood number was estimated using an empirical correlation for flow in cylindrical geometries.

$$Sh = 1.86 \left(Re^{\left(\frac{1}{3}\right)} Sc^{\left(\frac{1}{3}\right)} \right) \quad (3)$$

To further evaluate the mass transport characteristics within the upflow anaerobic hybrid reactor (UAHB), the Péclet number (Pe) [38] (Eq. 4) was calculated. This dimensionless number represents the ratio between convective and diffusive transport.

$$Pe = \frac{Lv}{D} \tag{4}$$

Where L is the characteristic length of the reactor (0.75 m), v is the average flow velocity (m s^{-1}), and D is the diffusivity of methane in water (1.3×10^{-9} m^2 s^{-1}).

The Péclet number provides insight into the relative importance of advective and diffusive transport within the reactor. A high Pe value suggests that advection dominates, while a low Pe value indicates a system with significant mixing and diffusion effects. This analysis is crucial for understanding mass transfer dynamics in anaerobic reactors, particularly for optimizing gas desorption and solute removal.

The Ergun equation [39] (Eq. 5) was applied to accurately estimate the pressure drop (ΔP) across the support media within the UAHB reactors. This equation is widely used to describe the flow behaviour in packed beds, considering both viscous and inertial pressure losses.

$$\Delta P = \frac{150(1-\varepsilon)^2}{\varepsilon^3}\frac{\mu v}{d_p^2} + \frac{1.75(1-\varepsilon)}{\varepsilon^3}\frac{\rho v^2}{d_p} \tag{5}$$

Where μ is the dynamic viscosity of the fluid (Pa·s), v is the superficial velocity (m s^{-1}), d_p is the equivalent particle diameter of the support media (m), ρ is the fluid density (kg m^{-3}), and ε is the bed porosity. This approach accounts for laminar and turbulent flow regimes, ensuring a more precise estimation of energy losses due to flow resistance within the structured PVC ring configuration. The calculated pressure drop provides insights into the hydrodynamic conditions within the reactors and their impact on mass transfer performance.

2.3. Support media of the UAHB reactors

The support media of the UAHB reactors consists of corrugated PVC rings (conduit type) with 2.0 cm diameter, 3.0 cm length, and 9.2 10^{-3} m^2 g^{-1} surface area [40], arranged to form hive-type modules to uniform the quantity and arrangement of the support media and promote microbial development and fixation, minimizing the loss of solids in the treated effluent.

Each module consists of 19 corrugated PVC rings arranged in concentric circles. Thus, to achieve the established heights for each reactor, two modules with a support medium height of 6 cm were included in UAHB reactor 1, five modules with a support medium height of 15 cm in UAHB reactor 2, and eight modules with a support medium height of 24 cm in UAHB reactor 3. The modules were installed at a distance of 40 cm measured from the bottom of each reactor, as shown in Figure 2.

Table 2. Composition of the synthetic wastewater.

Compound	Concentration (mg L^{-1})	Mass (mg) Vol. = 66.39 L d^{-1}
Meat Extract	240	15.93
Soluble Starch ($C_6H_{10}O_5$)	12	0.80
Wheat flour	240	15.93
Sucrose ($C_{12}H_{22}O_{11}$)	21	1.39
Ammonium Chloride (NH_4Cl)	91.2	6.05
Sodium chloride (NaCl)	300	19.92
Magnesium chloride (hexahydrate) ($MgCl_2$ $6H_2O$)	8.4	0.56
Calcium chloride ($CaCl_2$)	5.4	0.36
Potassium phosphate (KH_2PO_4)	15.84	1.05
Baking soda ($NaHCO_3$)	180	11.95

2.4. Inoculum

Before the operation, each UAHB reactor was inoculated with 1.5 L (approximately 27% of the total reactor volume) of anaerobic sludge from a pilot-scale UAHB reactor treating synthetic wastewater operated by Da Silva Ramos et al. [7], who analyzed its performance under temperature variations and methane recovery from the effluent. The inoculum presented average concentrations of total solids (TS), total fixed solids (TFS), and total volatile solids (TVS) of 47, 13, and 34 g L^{-1}, respectively.

2.5. Synthetic wastewater

The synthetic wastewater was prepared to simulate sanitary sewage, with the advantage of sanitary safety while performing laboratory analyses and maintaining controlled conditions [41]. Table 2 presents the composition of the synthetic wastewater for the concentration of approximately 500 mgCOD d^{-1}, equivalent to the organic loading rate (OLR) of 1.20 kgCOD m^{-3} d^{-1}, following the methodology adapted from Torres and Foresti [42]. The synthetic wastewater was prepared daily in volumes of 67 L.

2.6. Operating conditions

2.6.1. Adaptation phase and operation

The adaptation phase lasted 60 days, in which the UAHB reactors 1, 2, and 3 were continuously fed with synthetic wastewater at flowrates of 0.546, 0.538, and 0.531 L h^{-1}, respectively, and hydraulic retention time (HRT) of 10 h. The duration of the adaptation phase was determined according to the literature regarding startup periods and experimental control tests of anaerobic reactors [3,7,9].

The adaptation phase began after inoculating the UAHB reactors with anaerobic sludge from a pilot-scale UAHB reactor. This phase ended when the reactors reached the steady state verified by monitoring the physical–chemical parameters pH, alkalinity, volatile acids, and COD removal in influent and effluent samples of the reactors.

The results in the effluent samples indicated pH remaining close to 7.0, higher alkalinity compared to the influent, lower volatile acids (VA) compared to the influent, and COD removal efficiency exhibiting a consistent trend. Additionally, key stability indicators such as the intermediate/partial alkalinity (IA/PA), partial/total alkalinity (PA/TA), and VA/TA ratios fell within values reported by Ripley et al. and Jenkins et al. (IA/PA ≤ 0.3 [43], PA/TA ≥ 0.5 [44]; $0.1 \leq$ VA/TA ≤ 0.35 [43]).

After achieving the steady state, the reactors were continuously monitored throughout the 180-day experimental period by collecting influent and effluent samples four days per week at the same hour, minimizing external factors that could affect the performance of the reactors.

2.6.2. Monitoring parameters

Two months after inoculation, the performance of the reactors was evaluated in triplicate twice a week by determining the physical–chemical parameters of Table 3 in influent and effluent samples until reaching the steady state. Then, the physical–chemical parameters were determined in triplicate four times a week in influent and effluent samples of the reactors for four months.

During the research development, the daily gas volume generated in each UAHB reactor was monitored by a RITTER® MilliGascounters MGC-1 PMMA gas metre.

2.7. Statistical analysis

The Central Composite Design (CCD) method was applied to determine the best combination of the sizing parameters (cross-sectional area in m^2 and height in m) of the UAHB reactors and organic matter removal efficiency (%), with factorial runs (2^k), centre runs, and axial runs (2 k), in which k corresponds to the number of parameters.

The values of the parameters were obtained from the literature considering 42 studies from the period 2000–2022 regarding UAHB reactors filled with different support media and treating different wastewater (Table S1, Supplementary material).

Modelling and planning were conducted using the commercial software Statistica (version 10.0), considering the variables cross-sectional area (0.002–0.10 m^2), height (0.36–3.50 m), and organic matter removal efficiency (%). The variable parameters and their interactions were considered in a model to determine the highest organic matter removal efficiency for the UAHB reactors.

This method is suitable for process optimization, quadratic surface fitting, and interaction analysis between the investigated parameters, minimizing the number of experiments [47].

The results obtained in the physical–chemical characterization analyses of influent and effluent samples underwent statistical treatment considering measurement errors and errors in the systems (equipment) used. The standard error is obtained by multiplying the standard deviation by the Student's t-value (1.320) for three samples. Then, this result is divided by the square root of the number of samples (N) analyzed, as shown in Eq. 6.

$$\sigma m = \frac{\sigma p}{\sqrt{N}} \tag{6}$$

Where σp is the standard deviation, and N is the number of samples. The final errors associated with the different tests were obtained by combining the standard error with the systematic error provided by the instrument used for the measurements in each test, as described in Eq. 7.

$$Error = \sqrt{\sigma m^2 + \sigma s^2} \tag{7}$$

Where σm is the standard error, and σs is the systematic error. The significance was determined by analyzing how

Table 3. Parameters and methods applied in the study.

Parameters	Unit	Analysis method	Method number	Reference
Liquid temperature	C°	Thermocouple – Pt100 RTD Sensor	–	–
pH	–	Potentiometer	4500-H + B	[45]
Alkalinity (total, partial and intermediate)	$mgCaCO_3\ L^{-1}$	Titrimetric	–	[43]
Volatile Acids (VA)	$mgHAc\ L^{-1}$	Titrimetric	–	[46]
Turbidity	NTU	Turbidimetric	2130 B	[45]
Conductivity	$\mu S\ cm^{-1}$	Electrometric	2510	[45]
Chemical Oxygen Demand (COD)	$mgO_2\ L^{-1}$	Spectrophotometric	5220 D	[45]
Total Solids (TS)	$mg\ L^{-1}$	Gravimetric	1684	[45]
Total Fixed Solids (TFS)	$mg\ L^{-1}$	Gravimetric	1684	[45]
Total Volatile Solids (TVS)	$mg\ L^{-1}$	Gravimetric	1684	[45]

many times the error was smaller than the difference in the mean values of the results of each test performed. By obtaining the mean values and the associated errors, it was possible to compare the results within statistical certainties that ranged from 68.95 to 99%.

The data sets were analyzed using the Shapiro–Wilk test (Eq. 8) to determine the normality. This test can detect deviations from normality, whether due to asymmetry, kurtosis, or both [48].

$$W = \frac{\left(\sum_{i=1}^{n} a_i x_{(i)}\right)^2}{\sum_{i=1}^{n} (x_i - \bar{x})^2} \tag{8}$$

Where the variable X(i) represents the number occupying the i th position in the sample and the variable a_i represents independent and identically distributed random variables sampled from normal distributions. The data come from a normal distribution if the value of $p \geq 0.05$, i.e. H_0 is accepted.

The dependence or incidence of the support medium on COD removal variables was statistically established by Pearson's correlation coefficient when the variables presented a normal distribution.

Pearson [49] defines a measure of linear association between the two quantitative variables (discrete or continuous) X and Y. The correlation coefficient between random variables X and Y is shown in Eq. 9.

$$\sigma = \frac{\sum (x - \bar{x})(y - \bar{y})}{\sqrt{\sum (x - \bar{x})^2 \sum (y - \bar{y})^2}} \tag{9}$$

Variables with non-normal distribution were analyzed using Kendall's correlation test [50], named Kendall's τ (Tau), in which the correlation coefficient is calculated between variables X and Y (Eq. 10).

$$\mathrm{T} = \frac{2S}{n(n-1)} \tag{10}$$

The S variable represents the substruction between P and M, and the P variable represents the number of times the variable Y increments while X increments. Conversely, the M variable represents the number of times Y decreases while X increases.

The coefficients σ and Tau measure the linear relationship between the two variables, ranging from −1 to +1. The value −1 represents a perfect negative correlation, while the value +1 represents a perfect positive correlation.

Pearson and Kendall's interpretation of the correlation was made according to the magnitude ranges proposed by Evans [51]. Therefore, the correlation is considered 'very weak' when the value is in the range ± (0.00–0.19), 'weak' when the value is in the range ± (0.20–0.39), 'moderate' in the range ± (0.40–0.59), 'strong' in the range ± (0.60–0.79) and 'very strong' in the range ± (0.80–1.00). The sign accompanying the range indicates the possibility of a positive or directly proportional correlation and, otherwise, a negative or indirectly proportional correlation.

3. Results and discussion

3.1. Analysis of preliminary studies of UAHB reactors

Table S1 (Supplementary material) presents a summary of 42 studies from the period 2000–2022 regarding UAHB reactors filled with different support media and treating different wastewaters. The data were organized and filtered to process variables of sizing (cross-section area and height) and operation (organic matter removal efficiency) graphically (Figure 3).

The surface contains red regions representing organic matter removal greater than 76% in terms of COD. Yellow regions represent the reactors' cross-section and height, allowing removal efficiencies close to 56%. Green regions correspond to organic matter removals (COD) lower than 46%.

In order to identify the expected values of organic matter removal efficiency according to Figure 3, the value of the cross-section area of 0.007 m^2 was related to the red region at high organic matter removal. The dashed lines and the black arrow indicate that a reactor height of 0.75 m provided high organic matter removal for UAHB reactors with a cross-section area of 0.007 m^2.

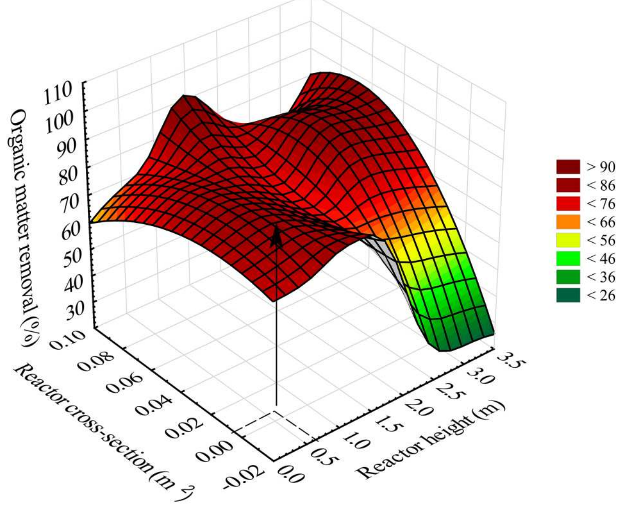

Figure 3. Three-dimensional response surface interaction effects of height (m) and cross-section area (m^2) of the UAHB reactors on the organic matter removal efficiency (% COD).

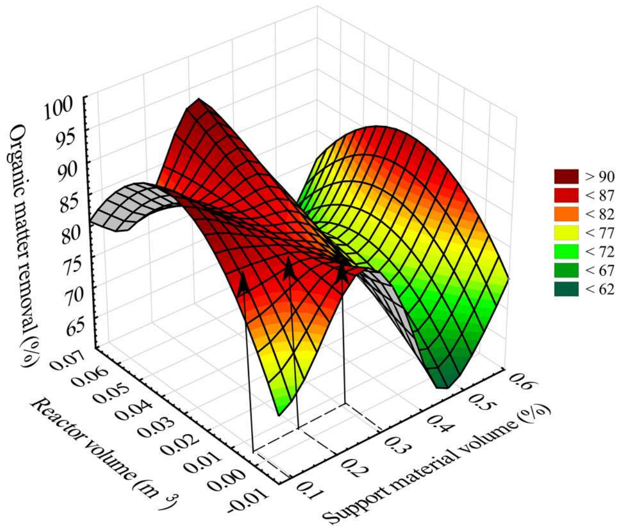

Figure 4. Three-dimensional response surface interaction effects of volume (m^3) and support material volume (%) of the UAHB reactors on the organic matter removal efficiency (% COD).

A height of 0.75 m was selected for the UAHB reactors to ensure consistency between the modelled and experimental results. Thus, this height was effectively implemented in the experimental setup. The subsequent experimental results confirmed that this geometric configuration led to high COD removal efficiencies, validating the model's predictions.

After defining the geometric sizing of the reactors and applying the same methodology of graph analysis, the variables reactor volume and support material volume inside the reactor were related to the variable organic matter removal efficiency in terms of COD (Figure 4).

The regions represent organic matter removal efficiencies greater than 87% (in red), close to 77% (in yellow), and lower than 72% (in green). The dashed lines and the black arrows indicate the heights of the support medium of 6, 15, and 24 cm, corresponding to 8, 20, and 32% of the total reactor volume, equivalent to 0.0055 m^3 used in this study. Thus, the best possibilities for organic matter removal are expected for this study.

3.2. UAHB reactor hydraulic characteristics

The hydrodynamic and mass transfer characteristics of the upflow anaerobic hybrid reactor (UAHB) were evaluated using dimensionless numbers and pressure drop analysis.

Considering a flow rate of 0.55, 0.54, and 0.53 L h^{-1} for UAHB reactors 1, 2, and 3, respectively, along with a water density of 998 kg m^{-3} and a dynamic viscosity of 1.002×10^{-3} Pa·s, the calculated Reynolds numbers were 1.94, 1.90, and 1.87 for UAHB 1, 2, and 3, respectively.

In the same way, based on Equations (2) and (3), the Schmidt number (Sc) and Sherwood number (Sh) were calculated to assess the mass transfer efficiency. The results obtained were 772.31 and 21.27 for UAHB 1, 772.31 and 21.14 for UAHB 2, and 772.31 and 21.01 for UAHB 3, respectively.

Based on Equation (4), the Péclet number (Pe) was calculated, resulting in 11,222.46 for UAHB 1, 11,018.42 for UAHB 2, and 10,814.37 for UAHB 3, respectively.

The pressure drop (ΔP) across the support media was calculated using the Ergun equation and considering the following parameters. The effective flow area through the support medium was determined to be 0.007242 m^2, while the support material density was 1.22 g cm^{-3}. The influent flow rates were 0.55 L h^{-1}, 0.54 L h^{-1}, and 0.53 L h^{-1} for UAHB reactors 1, 2, and 3, respectively. The porosity parameter was calculated based on the relationship between the filter material volume and the support media volume, as presented in supplemental material (Table S2. Characteristics of the Support Media). The water viscosity was estimated at 1.307×10^{-3} Pa·s.

Based on these values, the pressure drop (ΔP) across the support media was calculated as 0.0002 , 0.0005 , and 0.0008 Pa for UAHB reactors 1, 2, and 3, respectively.

The Reynolds number (Re) values for UAHB 1, 2, and 3 were 1.94, 1.90, and 1.87, respectively, confirming that the flow remains in the laminar regime ($Re < 2000$) [35]. This condition is expected in anaerobic reactors, where low velocities favour longer residence times and increased contact between biomass and substrate, improving organic matter degradation and biogas production [52]. The gradual decrease in Re follows the trend of declining flow rates (0.55, 0.54, and 0.53 L h^{-1}), which could indicate minor variations in hydrodynamic behaviour among the reactors.

The Schmidt number (Sc) remained constant at 772.31 for all reactors, as it depends solely on fluid properties (water density and viscosity). This high Sc value indicates that momentum diffusivity is significantly higher than mass diffusivity, meaning that convective transport dominates molecular diffusion [53]. The Sherwood number (Sh), representing the convective to diffusive mass transfer ratio, exhibited slight variations (21.27, 21.14, and 21.01 for UAHB 1, 2, and 3, respectively). It suggests that mass transfer efficiency slightly decreased as the flow rate declined, which aligns with the behaviour of the Reynolds number.

The Péclet number (Pe) values obtained (11,222.46, 11,018.42, and 10,814.37) confirm that advective transport is dominant over diffusive transport in all reactors [54]. The minor decrease in Pe across the reactors could indicate different dispersion characteristics within each system. These variations may be linked to subtle differences in biofilm formation, which can alter flow paths, substrate accessibility, and microbial activity [55].

The pressure drop across the support medium was calculated using the Ergun equation, yielding 0.0002 , 0.0005 , and 0.0008 Pa for UAHB 1, 2, and 3, respectively. The increase in pressure drop from UAHB 1 to UAHB 3 aligns with the decreasing flow rates and media support height increment, as lower velocities reduce shear stress and could favour higher biofilm accumulation within the support material [56].

3.3. Performance of the UAHB reactors

3.3.1. Analysis of control parameters

This study was conducted to verify the variation of the support medium height (SMH) on the performance of the UAHB reactors in terms of organic matter (COD) and removal efficiency, in addition to characterizing the physicochemical behaviour of the UAHB reactor for different support medium heights. Table 4 summarizes the results of liquid temperature, pH, alkalinity (partial, intermediate, and total), VA, turbidity, conductivity, COD, TS, TFS, and TVS in the influent and effluent samples of the UAHB reactors and biogas production.

The liquid temperature ranged from 13.4 to 20.5 °C in the influent samples during the operation, probably influenced by the variation of spring to summer seasons in which room temperatures varying from 10.2 to 27.7°C were measured by SIMEPAR [57]. In the effluent samples of the reactors, the liquid temperature varied from 13.5 to 21.2 °C in UAHB 1, 13.6–21.2 °C in UAHB 2, and 13.7–21.1 °C in UAHB 3, demonstrating no significant differences between the effluent samples (p-value = 0.90; 0.99; 0.91).

The liquid temperatures resulted lower than the range of 20–40 °C recommended by Metcalf and Eddy [58] and Foresti [42] for effective anaerobic digestion of sanitary sewage. In addition, Van Haandel et al. [59] noted that temperature directly impacts cellular metabolism, which decreases proportionally at lower temperatures, reducing biogas generation efficiency.

Psychrophilic anaerobic digestion, characterized by operational temperatures below 20 °C, is less common due to reduced microbial activity and decreased biogas production efficiency [60]. However, several studies have investigated the performance of anaerobic systems under these conditions. For instance, a comprehensive evaluation of a full-scale tubular digester operating for eight years at an average temperature of 17.7 °C demonstrated volatile solids reduction of approximately 77.6% and specific methane production of 0.40 N m^3CH_4 kg^{-1}VS, surpassing typical expectations for psychrophilic conditions [61].

In our study, the wastewater treatment occurred within the psychrophilic range. Similarly, Da Silva Ramos et al. [7] and Michelon et al. [9] analyzed temperature variations between 14 and 28°C and found no significant differences in methane production efficiency or chemical oxygen demand (COD) removal, suggesting that anaerobic systems can maintain stable performance even at lower temperatures and different hydraulic retention times (HRT). Similarly, Daija et al. [62] indicated that an extended hydraulic retention time helped mitigate the decline in methane production at psychrophilic temperatures.

By monitoring biogas production in a UAHB reactor, Michelon et al. [9] indicated that the support medium mitigated fluctuations associated with temperature drops, as the fixed bed compensated for the instability of the moving bed. Da Silva Ramos et al. [7] suggested that hybrid reactors with support media could capture more methane from dissolved gas, thereby improving overall system efficiency at any temperature.

The findings from our study align with previous research, demonstrating the feasibility of anaerobic digestion under psychrophilic conditions.

The pH values varied from 6.4 to 7.5 in the influent samples and the effluent samples from 6.1 to 7.5 for UAHB 1, 6.2–7.8 for UAHB 2, and 6.4–7.5 for UAHB 3. These results are in the range recommended by Hoyos [63] and Wang [64], who indicated that maintaining pH between 6.0 and 8.5 boosts the development and activity of bacterial groups in the biomass, enhancing the anaerobic digestion efficiency. Additionally, the pH varying from 6.5 to 7.5 could favour methanogenic archaea growth, according to Qiu et al. [65], Kullavanijaya et al. [66], and Sun et al. [67]. No significant differences were noted between the effluent samples (p-value = 0.24; 0.60; 0.43), presenting a neutrality tendency.

Some authors indicated that the support material height and reactor configuration could influence pH stability during operation. For example, Silva et al. [35] monitored pH levels (6.73–7.34) during the operation on a UAHB reactor (3,107 L) with a height of 4.0 m and a support material height of 1.0 m, noting that the system demonstrated buffering capacity and maintained stable pH conditions treating coffee wastewater. Moreover, Araujo et al. [68] observed pH levels ranging from 5.8 to 8.0 in a UAHB reactor (16.3 L) with a height of 0.8 m and support material height of 0.4 m treating household and personal products industry wastewater.

Table 4. Physicochemical characterization of the influent and effluents from the reactors UAHB 1 (SMH = 6 cm), 2 (SMH = 15 cm), and 3 (SMH = 24 cm).

Parameter	Unit	Samples	Average	Removal (%)	SD	CV	Min.	Max.
Liquid temperature	C°	Influent	17.9	–	2.2	12.2	13.4	20.5
		UAHB 1	18.4	–	2.3	12.6	13.5	21.2
		UAHB 2	18.3	–	2.3	12.3	13.6	21.2
		UAHB 3	18.3	–	2.2	12.2	13.7	21.1
pH	-	Influent	6.8	–	0.3	3.9	6.4	7.5
		UAHB 1	6.9	–	0.3	4.9	6.1	7.5
		UAHB 2	7.0	–	0.4	5.3	6.2	7.8
		UAHB 3	7.0	–	0.3	4.2	6.4	7.5
Partial alkalinity	$mgCaCO_3\ L^{-1}$	Influent	114	–	28	25	58	173
		UAHB1	133	–	16	12	107	168
		UAHB2	135	–	19	14	105	181
		UAHB3	136	–	24	18	73	173
Intermediate alkalinity	$mgCaCO_3\ L^{-1}$	Influent	63	–	33	52	8	130
		UAHB1	70	–	25	36	27	122
		UAHB2	79	–	28	35	11	131
		UAHB3	80	–	29	36	15	135
Total alkalinity	$mgCaCO_3\ L^{-1}$	Influent	176	–	59	34	77	304
		UAHB1	203	–	37	18	136	290
		UAHB2	214	–	45	21	138	312
		UAHB3	216	–	53	24	88	307
Volatile Acids	$mgHAc\ L^{-1}$	Influent	54	–	16	30	25	77
		UAHB1	63	–	27	43	31	129
		UAHB2	62	–	24	38	30	130
		UAHB3	58	–	15	26	31	88
Turbidity	NTU	Influent	61	–	5	9	52	70
		UAHB1	9	85	5	54	3	16
		UAHB2	8	87	2	25	5	13
		UAHB3	6	90	2	28	3	10
Conductivity	$\mu S\ cm^{-1}$	Influent	1101	–	64	6	962	1180
		UAHB1	1105	–	59	5	967	1176
		UAHB2	1109	–	63	6	957	1221
		UAHB3	1113	–	63	6	954	1198
COD	$mgO_2\ L^{-1}$	Influent	490	–	53	11	416	592
		UAHB1	154	69	74	48	68	271
		UAHB2	146	70	44	30	95	257
		UAHB3	138	72	48	35	66	242
TS	$mg\ L^{-1}$	Influent	771	–	49	6	683	833
		UAHB1	304	61	40	13	259	362
		UAHB2	287	63	35	12	238	337
		UAHB3	285	63	35	12	245	339
TFS	$mg\ L^{-1}$	Influent	535	–	62	12	414	605
		UAHB1	205	62	33	16	167	251
		UAHB2	209	61	38	18	172	265
		UAHB3	200	63	34	17	168	257
TVS	$mg\ L^{-1}$	Influent	235	–	52	22	185	335
		UAHB1	98	58	26	26	64	134
		UAHB2	77	67	22	29	61	117
		UAHB3	85	64	27	32	69	134
Biogas production	$NL\ L^{-1}$	UAHB1	1,3	–	0,1	9,1	1,1	1,6
		UAHB2	1.1	–	0,2	11,5	1,2	1,7
		UAHB3	0.5	–	0,1	9,4	1,4	1,9

Note: SD – standard deviation; CV – coefficient of variation; n – number of samples = 54.

The average total alkalinity of 176 ± 59 $mgCaCO_3\ L^{-1}$ in the influent samples, varying from 77 to 304 $mgCaCO_3\ L^{-1}$ (Figure 5), resulted closer to the maximum value of the range 110–170 $mgCaCO_3\ L^{-1}$ for sanitary sewage characterized Metcalf & Eddy [58] and Sperling [69].

The increase of 10%, 14%, and 15% corresponding to the total bicarbonate alkalinity of 203 ± 37, 214 ± 45, and 216 ± 53 $mgCaCO_3\ L^{-1}$ for the effluent samples of UAHB 1, 2, and 3, respectively, indicate the buffering capacity of these reactors and the stability of the process. Foresti et al. [42] stated that the increment in alkalinity is a common indicator of treatment stability. No significant differences (p-value = 0.42; 0.88; 0.38) were observed by comparing the effluent samples of the reactors, suggesting that the support medium height did not influence this parameter.

The presence of support materials has shown improved biomass retention and, consequently, the microbial activity responsible for alkalinity production. The interaction between support materials facilitates the growth of methanogenic archaea that utilize the intermediate acids produced during anaerobic digestion, augmenting alkalinity generation [70–72].

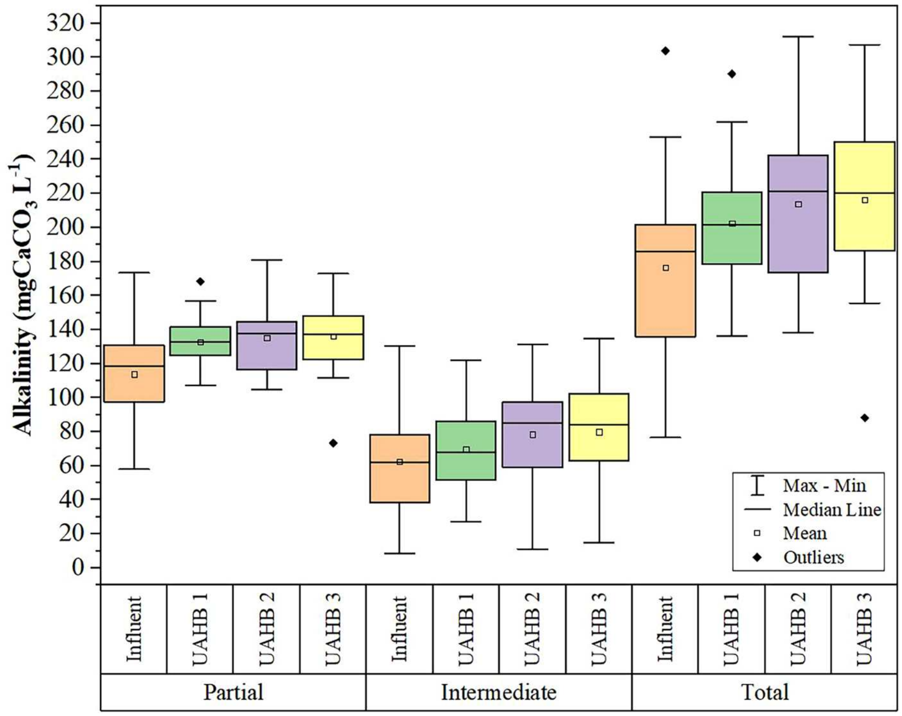

Figure 5. Variation of Alkalinity (Partial, Intermediate, and Total, $mgCaCO_3$ L^{-1}) in the UAHB reactors: 1 (SMH = 6 cm), 2 (SMH = 15 cm), and 3 (SMH = 24 cm).

Average partial (PA) and intermediate alkalinities (IA) of 114 ± 28 and 63 ± 33 $mgCaCO_3$ L^{-1} for the influent samples, and 133 ± 16 and 70 ± 25 $mgCaCO_3$ L^{-1}, 135 ± 19 and 79 ± 28 $mgCaCO_3$ L^{-1}, and 136 ± 24 and 80 ± 29 $mgCaCO_3$ L^{-1} for the effluent samples of UAHB 1, 2, and 3 reactors, respectively (Figure 5), reinforced the buffering capacity of these reactors, independently of the height of the support media adopted. No significant differences were obtained between the results obtained for PA and IA of effluent samples (p-value = 0.70; 0.88; 0.62), suggesting that the height of the support medium did not influence these parameters.

Ripley et al. [43] stated that the IA/PA ratio exceeding 0.3 suggests potential disturbances in anaerobic digestion. In our study, average IA/PA ratios were 0.52 ± 0.20 for UAHB 1, 0.58 ± 0.22 for UAHB 2, and 0.59 ± 0.24 for UAHB. Conversely, Foresti [73] argues for a closer examination of this threshold and indicates that stability could be achieved with IA/PA ratio values above 0.3. In addition, Silva and Nour [74] achieved satisfactory removal efficiencies of COD (73.7%) and Total Suspended Solids (78.8%) with IA/PA ratios ranging from 0.47 to 1.12 in a compartmentalized anaerobic reactor treating urban wastewater with initial COD of 790 mgO_2 L^{-1} and TSS of 279 mg L^{-1}. The IA/PA ratio values obtained in our study align with those mentioned by Silva and Nour [74], indicating favourable conditions in the anaerobic treatment process.

Despite indicating reduced buffering capacity for AI/PA values between 0.40 and 0.80, Souza et al. [75] noted that stability could be achieved even with AI/PA ratios greater than 0.30. These results are consistent with our findings that the reactors demonstrated satisfactory COD removal efficiencies even with the observed AI/PA ratios. Furthermore, Pereira et al. [71] reported that high AI/PA ratios do not necessarily correlate with the poor performance of a UASB reactor treating swine wastewater. In conclusion, anaerobic digestion can be effective even under varying alkalinity conditions.

Moreover, the PA/TA ratio is recommended to indicate stability in anaerobic treatment, with effective organic matter removal and methane production. Pérez and Torres [76] mentioned maintaining the PA/TA ratio above 0.65, and Jenkins et al. [44] stated that this ratio should surpass 0.5. López-López et al. [72] reported that PA/TA ratios consistently above 0.5 indicate a well-buffered system capable of neutralizing volatile acids produced during anaerobic digestion. Santana and Oliveira [77] maintained PA/TA ratios around 0.47–0.60 without significant operational disturbances. In our study, the PA/TA ratio is in agreement with these referenced studies since the average values resulted in 0.66 ± 0.34 for UAHB 1, 0.64 ± 0.40 for UAHB 2, and 0.67 ± 0.48 for UAHB 3, demonstrating the stability potential of these reactors even with different heights of support media.

Volatile acids ranged from 25 to 77 mgHAc L^{-1} in the influent samples, resulting in an average concentration of 54 ± 16 mgHAc L^{-1}. These concentrations agree with the range that Torres & Foresti [42] indicated of 25–110 mgHAc L^{-1} for sanitary sewage. Similar concentrations were verified in the effluent samples, resulting in 63 ± 27 mgHAc L^{-1} for UAHB 1, 62 ± 24 mgHAc L^{-1} for UAHB 2, and 58 ± 15 mgHAc L^{-1} for UAHB 3 (Figure 6). The support media increase the contact time between substrate and biomass, minimizing the accumulation of VA and enhancing hydrogen production, as reported by Hernandez et al. [78] in hybrid UASB-type reactors filled with Biopack® rings.

In anaerobic digestion, volatile fatty acids (VFAs) typically range from 50 to 250 mgHAc L^{-1}, creating favourable conditions for methanogenic archaea to convert intermediate products into methane and carbon dioxide efficiently [79]. However, not all VFAs are degraded at the same rate. Short-chain VFAs, such as acetate, are more readily utilized by methanogens, whereas propionate and butyrate require specific microbial pathways and may accumulate if degradation is hindered [80,81]. In our study, the concentrations of VFAs observed in the effluent samples from the UAHB reactors were within the expected range. The presence of carbohydrates and proteins in the synthetic wastewater composition suggests that propionate and butyrate could form intermediate fermentation products. However, no significant accumulation was observed, indicating that the process conditions facilitated their further conversion.

By comparing the VA concentrations between the influent and effluent samples, no significant differences were noted (p-values = 0.91; 0.55; 0.50), indicating no accumulation and neutralization of VA during the operation of the UAHB reactors. Thus, the height of the support medium did not influence this parameter.

Ripley et al. [43] indicated that the efficiency of anaerobic digestion is closely linked to the concentrations and interaction between Total alkalinity (TA) and Volatile acids (VA). In addition, these authors suggest optimal organic matter degradation for the VA/TA ratio ranging between 0.1 and 0.35. In our study, the VA/TA ratios resulted in 0.31 ± 0.14 for UAHB 1, 0.29 ± 0.13 for UAHB 2, and 0.27 ± 0.10 for UAHB 3, i.e. demonstrating conditions for the organic matter degradation in anaerobic treatment.

Figure 7 shows the turbidity (UNT) variation in the influent and effluent samples and the removal efficiencies (%) achieved by UAHB reactors.

The average turbidity in the influent samples resulted in 61 ± 5 NTU, a value close to the result of Godinho [10] (59 UNT) when using synthetic sewage with a similar composition. In the effluent samples, the turbidity presented values of 9 ± 5, 8 ± 2, and 6 ± 2 NTU for UAHB 1, 2, and 3, respectively, indicating that the higher the support media height, the lower the turbidity.

UAHB reactors 1, 2, and 3 achieved average turbidity removals of 85.2 ± 19.3%, 86.9 ± 14.9%, and 90.2 ± 14.9% for HRT of 10 h, respectively. The height of the support medium influenced the turbidity removal since the highest removal was verified in the UAHB 3, with the highest support medium height of 24 cm.

Electrical conductivity of 1,101 ± 64 µS cm^{-1} was measured in the influent samples, and 1,105 ± 59, 1,109 ± 63, and 1,113 ± 63 µS cm^{-1} were obtained in the effluent samples of the UAHB reactors 1, 2, and 3,

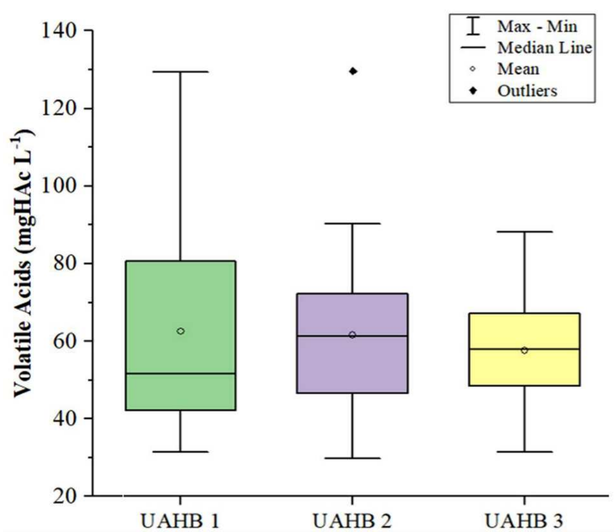

Figure 6. Variation of volatile acids (mgHAc L^{-1}) concentration in the UAHB reactors: 1 (SMH = 6 cm), 2 (SMH = 15 cm), and 3 (SMH = 24 cm).

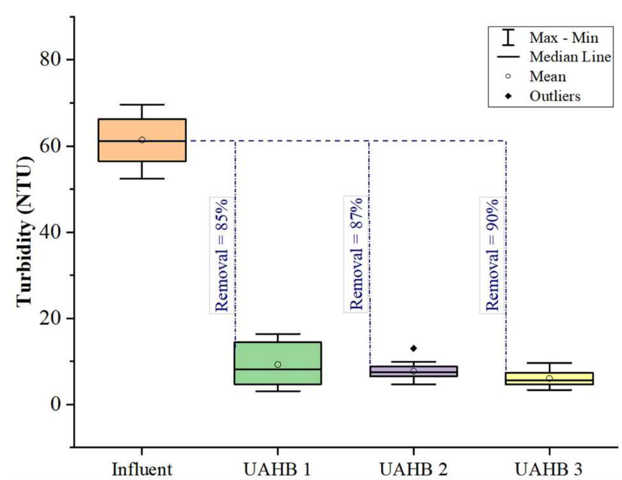

Figure 7. Variation of Turbidity (NTU) and removal efficiencies (%) achieved by the UAHB reactors: 1 (SMH = 6 cm), 2 (SMH = 15 cm), and 3 (SMH = 24 cm).

respectively. These results range from 550 to 1,330 µS cm^{-1}, as suggested by Liang et al. [82] for the electrical conductivity of typical sanitary sewage.

Higher electrical conductivity values were achieved in the UAHB 3 with higher support medium height (24 cm), probably due to the greater solids retention in the support medium and greater quantity of adhered biomass in this reactor. In the metabolization process of microorganisms, large molecules are transformed into small molecules with an electrical charge, increasing the conductivity of the medium [83,84]. Thus, the amount of microorganisms adhered to the surface is related to the conductivity measurement.

Conductivity plays an important role in monitoring and controlling anaerobic digestion processes since the concentration of ions is related to bacterial activity [85]. In our study, the higher electrical conductivity in UAHB 3 may indicate greater bacterial activity in this reactor compared to UAHB 1 and 2.

Figure 8 shows the organic matter concentrations (mg L^{-1}) regarding COD and the removal efficiencies (%) achieved by the UAHB reactors.

UAHB 1, 2, and 3 reactors achieved COD removal efficiencies of 69.4 ± 10.1%, 70 ± 6.6%, and 72.6 ± 7.5% for the initial concentration of 490 ± 53 mgO_2 L^{-1}, respectively, corresponding to the remaining concentrations of 154 ± 74, 146 ± 44 and 138 ± 48 mgO_2 L^{-1}. Sanitary sewage with an average COD concentration of 490 ± 53 mgO_2 L^{-1} falls within the medium to high concentration range according to Metcalf & Eddy's classification [58].

The height of the support medium did not influence COD removal efficiency since no statistical differences

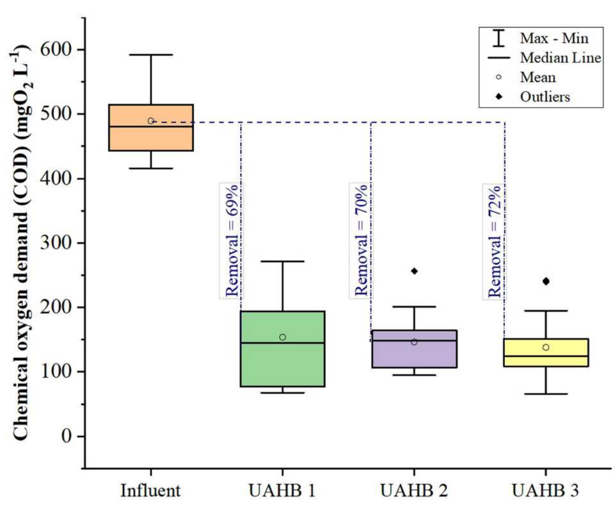

Figure 8. Organic matter concentrations (COD, mgO_2 L^{-1}) and removal efficiencies (%) achieved by the UAHB reactors: 1 (SMH = 6 cm), 2 (SMH = 15 cm), and 3 (SMH = 24 cm).

(p-value = 0.72; 0.59; 0.46) were observed between the effluent samples of these reactors.

Elmitwalli et al. [29], Godinho [10], Priya et al. [25], Loganath and Mazumder [86], Michelon et al. [9], Hemalatha and Keerthinarayana [87], Balasundaram et al. [88], and Da Silva et al. [7] obtained similar results in UAHB reactors treating sanitary sewer, synthetic sewer simulating sanitary sewer, sago processing wastewater, slaughterhouse effluent, paper manufacturing wastewater, and food processing wastewater.

Notably, the removal efficiencies obtained in the monitoring analyses agree with the results of preliminary studies (Figures 3 and 4), which were used to design and dimension the UAHB reactors and establish the operational conditions of our study. Thus, the experimental behaviour of the UAHB reactors corresponds to the expected behaviour according to the literature review.

Figure 9 shows the concentrations of total solids, total fixed solids, and total volatile solids (mg L^{-1}) and the removal efficiencies (%) in the UAHB reactors. Average Total solids (TS) of 771 ± 49 mg L^{-1} corresponds to the typical value for sanitary sewage, according to Metcalf et al. [58], who indicated the range from 390 and 1350 mg L^{-1} and Sperling [69], who suggested the range of 700–1350 mg L^{-1}.

The height of the support medium did not influence the removal efficiencies of TS (p-value 0.51; 0.96; 0.51) since UAHB 1, 2, and 3 reactors achieved similar average removal efficiencies with 61 ± 1%, 63 ± 2%, and 63 ± 2%, respectively. Similarly, no significant differences were noted between the total fixed solids (TFS) concentrations in the effluent samples of the reactors (p-value 0.90; 0.76; 0.85).

Regarding Total Volatile Solids (TVS), UAHB 2 and 3 reactors achieved higher removal efficiencies (67 ± 16% and 64 ± 16%) compared to UAHB 1 reactor (58 ± 15%), indicating that the higher support medium heights (SMH = 15 and 24 cm) influenced the TVS removal efficiency (p-value 0.04; 0.55; 0.35). Da Silva et al. [7] and Michelon et al. [9] achieved TVS removal efficiencies from 68–82% in UAHB reactors treating synthetic sewage with characteristics similar to our study.

Figure 10 shows the biogas production (NL L^{-1}) in the UAHB reactors.

The average values of biogas production were equal to 1.3 ± 0.1 NL d^{-1}, 1.5 ± 0.2 NL d^{-1}, and 1.6 ± 0.1 NL d^{-1} for UAHB reactors 1, 2 and 3. The height of the support medium influenced biogas production since statistical differences (p-value = 0.01; 0.00; 0.01) were observed between the effluent samples of these reactors.

According to Van Haandel et al. [59], anaerobic digestion occurs through the metabolic action of various

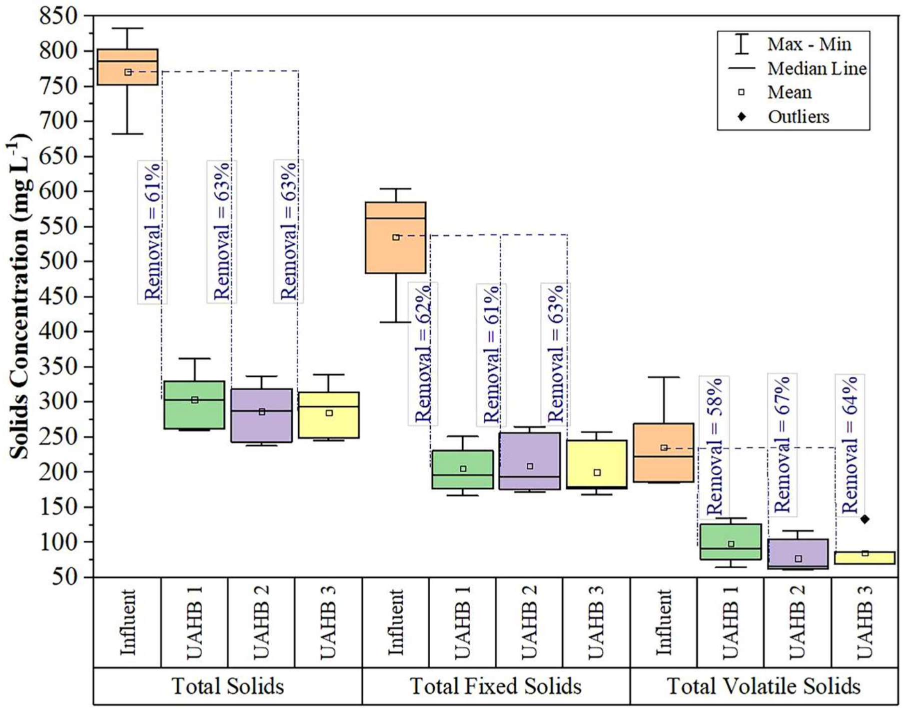

Figure 9. Solids concentrations (total, fixed, and volatile) and removal efficiencies (%) in the UAHB reactors: 1 (SMH = 6 cm), 2 (SMH = 15 cm), and 3 (SMH = 24 cm).

anaerobic microorganisms, transforming organic matter and producing biogas as a byproduct. Consequently, biogas production is influenced by biomass retention inside the reactor [89]. Based on this premise, it was expected that increasing the thickness of the support medium would enhance biogas production. This hypothesis was supported by the monitoring results, which indicated that the highest biogas production occurred in the UAHB 3 reactor, which had a support medium thickness of 24 cm.

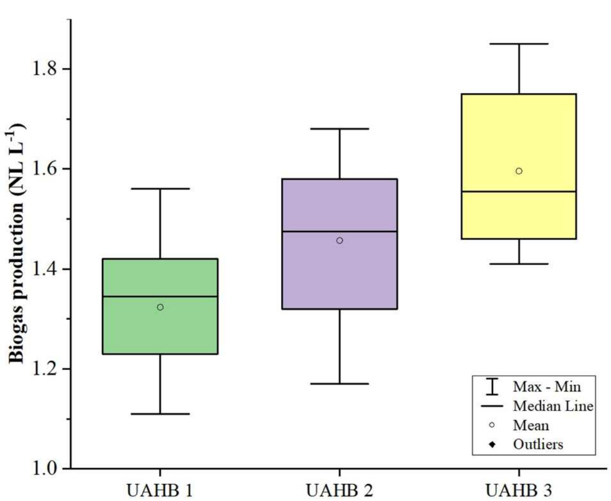

Figure 10. Biogas production in the UAHB reactors: 1 (SMH = 6 cm), 2 (SMH = 15 cm), and 3 (SMH = 24 cm).

Notably, the overall trend of biogas production in the three reactors follows the same pattern as organic matter removal regarding COD, demonstrating that greater organic matter removal is associated with increased biogas production.

The results of physicochemical parameters reinforce the influence of support media and the hydrodynamic conditions on reactor performance. The pH values increased slightly from 6.8 in the influent to 6.9, 7.0, and 7.0 in the effluent samples of UAHB 1, 2, and 3, respectively, reflecting the buffering capacity due to the alkalinity generation. Total alkalinity increased from 176 mg$CaCO_3$ L^{-1} in the influent to 203, 214, and 216 mg$CaCO_3$ L^{-1} in the effluent of these reactors, respectively, which is crucial for maintaining the reactor stability and preventing acidification.

The removal efficiency of COD improved progressively (69%, 70%, and 72%), correlating with the decreasing Pe and Sh values, suggesting that longer residence times favoured substrate degradation. Turbidity removal followed a similar trend (85%, 87%, and 90%), supporting the influence of mass transfer characteristics on particle retention and microbial activity.

3.3.2. Optimization

Statistical correlation analyses were developed after the general analysis of the experimental results.

Table 5. Results of the p-value of the Shapiro-Wilk normality test for the physicochemical parameters of the UAHB reactors: 1 (SMH = 6 cm), 2 (SMH = 15 cm), and 3 (SMH = 24 cm).

Parameter	*p*-value			
	Synthetic wastewater	UAHB 1	UAHB 2	UAHB 3
Temperature	0.125	0.155	0.248	0.198
pH	0.930	0.660	0.697	0.562
Partial alkalinity	0.967	0.687	0.542	0.397
Intermediate alkalinity	0.924	0.685	0.325	0.949
Total alkalinity	0.780	0.687	0.542	0.397
Volatile Acids	0.391	0.807	0.581	0.815
Turbidity	0.465	*0.037*	0.064	*0.038*
Conductivity	0.182	*0.008*	0.304	0.423
COD	0.087	0.070	0.073	*0.047*
TS	0.386	0.109	0.218	*0.024*
TFS	0.238	*0.010*	0.059	*0.007*
TVS	0.111	*0.015*	*0.009*	*0.009*
Biogas production	–	0.706	0.268	*0.038*

Table 5 presents the *p-value* results of the Shapiro–Wilk test (normality test).

The Shapiro–Wilk normality analysis showed that most of the data sets correspond to the characteristics of normal distribution because the *p-value* results are higher than 0.05 (significance level). However, results of turbidity, COD, TS, TFS, TVS, and Biogas production present non-normal distribution characteristics as the *p-value* results are lower than 0.05, thus rejecting the null hypothesis H_0 (there is no correlation between the height of the support medium and the tested monitoring parameter).

Then, the Pearson's correlation test was applied for the parameters that followed the normal distribution of the Shapiro–Wilk test, and the Kendall correlation test was applied for the parameters that did not follow the normal distribution of the Shapiro–Wilk test.

Table 6 shows the Pearson's correlation coefficient (σ) results between the different heights of the support medium and the operating parameters. The Person's correlation coefficient (σ) was calculated to establish the dependence of each parameter with the variable height of the support medium, considering a null hypothesis (H_0, in which there is no correlation between the height of the support medium and the tested monitoring parameter: $\sigma = 0$) and an alternative hypothesis (H_1, in which there is a correlation between the height of the support medium and the tested monitoring parameter: $\sigma \neq 0$).

Pearson's correlation results indicated a positive correlation between the support medium height and the pH, alkalinity (partial, intermediate, and total), and conductivity parameters. A negative correlation exists between the support medium height, temperature, and volatile acids. These correlations could be classified as 'very strong' except for the pH, which presents a 'moderate' correlation following Evans's classification [51].

Table 7 shows Kendall's correlation results for the parameters that did not follow a normal distribution. Kendall's non-parametric correlation test was developed to establish the dependence on the variable height of the support medium, considering a null hypothesis (H_0, in which there is no correlation between the height of the support medium and the tested monitoring parameter: $T = 0$) and an alternative hypothesis (H_1, in which there is a correlation between the height of the support medium and the tested monitoring parameter: $T \neq 0$).

Kendall's correlation results indicated a 'very strong' negative correlation between the turbidity, COD, and TS parameters. On the other hand, the results indicated a 'very strong' positive correlation between the support media height and the biogas production parameter and a 'weak' negative correlation between the TFS and TVS parameters, according to Evans's classification [51].

The study results indicate that the UAHB 3 reactor, with the highest support medium height (24 cm), exhibited the greatest values for electrical conductivity, biogas production, and total volatile solids (TVS) removal. These findings suggest a direct relationship between the support medium height and bacterial activity inside the reactor [5,73,85].

Higher electrical conductivity in UAHB 3 can be attributed to increased solids retention within the support medium and the higher amount of adhered biomass. Since conductivity is linked to ion concentration, it represents an important indicator of microbial activity [85]. This observation is further supported by Pearson's

Table 6. Pearson's correlation coefficient (σ) between support medium height and the operational parameters in UAHB reactors: 1 (SMH = 6 cm), 2 (SMH = 15 cm), and 3 (SMH = 24 cm).

Parameter	UAHB 1	UAHB 2	UAHB 3	σ	Correlation interpretation*	*p-value*
Temperature	18.4	18.3	18.3	−0.8	Very strong	0.40
pH	6.9	7.0	7.0	0.6	Moderate	0.60
Partial alkalinity	133	135	136	1.0	Very strong	0.14
Intermediate alkalinity	70	79	80	0.9	Very strong	0.25
Total alkalinity	203	214	216	0.9	Very strong	0.22
Volatile Acids	63	62	58	−0.9	Very strong	0.22
Conductivity	1105	1109	1113	1.0	Very strong	0.04

Note: * Evans [51].

Table 7. Kendall's correlation coefficient (T) between the support medium height and the operational parameters in UAHB reactors: 1 (SMH = 6 cm), 2 (SMH = 15 cm), and 3 (SMH = 24 cm).

Parameter	UAHB 1	UAHB 2	UAHB 3	T	Correlation interpretation	*p-value*
Turbidity	9	8	6	−1.0	Very strong	0.12
COD	154	146	138	−1.0	Very strong	0.12
TS	304	287	285	−1.0	Very strong	0.12
TFS	205	209	200	−0.3	Weak	0.60
TVS	98	77	85	−0.3	Weak	0.60
Biogas Production	1.32	1.45	1.59	1.0	Very strong	0.12

Note: * Evans [51].

correlation analysis, indicating a very strong positive correlation between support medium height and electrical conductivity and alkalinity (partial, intermediate, and total). Considering that alkalinity is closely associated with microbial metabolism and system stability [85,90], these findings reinforce the hypothesis that a higher support medium height enhances microbial retention and activity.

Although no statistical differences were observed in COD removal efficiency among the reactors, the higher removal in UAHB 3 may be associated with greater biomass retention and metabolic activity. Previous studies have demonstrated that the retention of microorganisms in the support medium [59] influences the efficiency of organic matter degradation in anaerobic systems. Kendall's correlation results corroborated this relationship, indicating a very strong negative correlation between support medium height and turbidity, COD, and total solids (TS). It suggests that higher support medium height promotes greater removal of these parameters, likely due to enhanced microbial degradation and solids entrapment.

Regarding total solids, the removal efficiencies for total fixed solids (TFS) were similar across the reactors, indicating that the support medium height did not significantly impact this parameter. However, the removal of total volatile solids (TVS) was higher in UAHB 2 and 3 compared to UAHB 1, suggesting that a higher support medium height could enhance the retention and degradation of biodegradable organic fractions. Nevertheless, Kendall's correlation results indicated a weak negative correlation between support medium height and TFS/TVS, suggesting that other operational factors may influence solids removal efficiencies.

Biogas production corroborates these findings, as UAHB 3 exhibited the highest biogas generation, with significant differences from the other reactors. Since biogas production is directly linked to microbial activity and biomass retention [91], the increased production in UAHB 3 confirms that the higher support medium height favoured microbial growth and metabolism. Pearson's and Kendall's correlation analyses strongly supported this relationship, which classified the correlation between support medium height and biogas production as very strong and positive.

In summary, the results collectively suggest that the increased height of the support medium in UAHB 3 contributed to enhanced microbial retention and activity, leading to greater organic matter degradation, higher volatile solids removal, increased electrical conductivity, and improved biogas production. The correlation analyses further reinforce these findings, demonstrating that key parameters such as alkalinity, conductivity, and biogas production are positively associated with support medium height. Besides turbidity, COD and total solids exhibit a strong negative correlation. These findings highlight the importance of support media height in optimizing anaerobic reactor performance and support the premise that greater bacterial activity is associated with increased biogas yields and organic matter conversion efficiency.

3.4. Limitations of the present study

The findings of this study offer several practical implications. The results suggest that optimizing the support medium height (SMH) in UAHB reactors can improve biomass retention and organic matter removal efficiency, reducing the pollutants released into water bodies and contributing to better water quality and overall ecosystem health.

This optimization could be implemented in full-scale reactors to enhance their performance, potentially leading to more efficient wastewater treatment systems. Although the findings of this study provide valuable insights, the practical implementation of these results may be subject to site-specific conditions, including variations in wastewater composition, reactor scale, and operational practices.

Challenges remain in optimizing the UAHB reactors on a full scale, particularly in ensuring long-term operational stability and minimizing environmental impacts associated with reactor maintenance and operation. Further studies must assess these findings in full-scale units regarding their applicability and limitations.

4. Conclusions

The UAHB reactors operated at HRT of 10 h maintained stable and neutral pH conditions and buffering capacity, demonstrating the stability of the anaerobic process even with different heights of the support medium. The support media improved the retention and activity of biomass responsible for alkalinity production, with greater values (216 ± 53 $mgCaCO_3$ L^{-1}) in the effluent of the UAHB reactor with higher support media height (SMH = 24 cm).

The UAHB reactors 1 (6 cm), 2 (15 cm), and 3 (24 cm) removed 85 ± 19%, 87 ± 15%, and 90 ± 15% of turbidity, indicating that the higher the support media height, the lower the remaining turbidity.

Although the support media height (SMH) showed differences in COD and TS removal efficiencies, these differences were not statistically significant to establish a direct influence on these parameters. However, the UAHB reactor with the highest SMH (24 cm) achieved removal efficiencies of 72.6 ± 7.5% for COD and 63 ± 2% for TS. These findings confirmed the hypothesis that increasing the height of the support medium in the UAHB reactor improves biomass retention and organic matter removal efficiency.

The Central Composite Design (CCD) results suggested that with a cross-sectional area of 0.007 m^2 and a height of 0.75 m to achieve COD removal efficiencies in the 72 - 87% range. The experimental results (COD removal efficiencies = 69 ± 10%, 70 ± 7%, 72 ± 8% for UAHB 1, UAHB 2, and UAHB 3, respectively) with the UAHB reactors were close to this expected range, supporting the design approach based on the CCD methodology.

Turbidity, volatile acids, COD, and total solids (fixed and volatile) showed a 'very strong' negative correlation with the support medium height. The correlation was classified as 'moderate' negative for total fixed and volatile solids. Conversely, biogas production and alkalinity exhibited a 'very strong' positive correlation with the support medium height.

Acknowledgments

The authors thank the support of the Coordination for the Improvement of Higher Education Personnel (CAPES) [Finance code 001]. We also thank the anonymous reviewers for their valuable contributions.

Disclosure statement

The authors declare that they have no known competing financial interests or personal relationships that could have appeared to influence the study reported in this manuscript.

Data availability statement

The authors confirm that the data supporting the findings of this study are available within the article and/or in its supplementary materials.

ORCID

Alvaro Javier Esteban Villota Mora http://orcid.org/0000-0002-5001-7551
Yeimy Ordoñez Muñoz http://orcid.org/0000-0002-8166-8867
Eduardo Borges Lied http://orcid.org/0000-0002-4680-5248
Vsevolod Mymrin http://orcid.org/0000-0002-1776-992X
Karina Querne de Carvalho http://orcid.org/0000-0003-4577-7537
Fernando Hermes Passig http://orcid.org/0000-0002-7461-0616

References

[1] Sathyamoorthy GL. Substrate removal kinetics for anaerobic hybrid reactor (AHR) treating dairy industrial wastewater. Int J Recent Technol Eng. 2019;7(4):234–240.
[2] Omil F, Garrido JM, Arrojo B, et al. Anaerobic filter reactor performance for the treatment of complex dairy wastewater at industrial scale. Water Res. 2003;37(17):4099–4108. doi:10.1016/S0043-1354(03)00346-4
[3] Patel BB, Rana PH. Performance evaluation of hybrid upflow anaerobic sludge blanket reactors with different inert media for sewage treatment. Bioresource Technol Rep. 2022;18:101075. doi:10.1016/j.biteb.2022.101075
[4] Da Silva VG, Campos CMM, Pereira EL, et al. Characterization of the biomass of a hybrid anaerobic reactor (HAR) with two types of support material during the treatment of the coffee wastewater. Braz Arch Biol Technol. 2013;56(3):495–504. doi:10.1590/S1516-89132013000300018
[5] Chernicharo CAL. Anaerobic reactors. Water Intel Online. 2015;6(0):9781780402116–9781780402116. doi:10.2166/9781780402116
[6] Zinatizadeh AA, Mohammadi P, Mirghorayshi M, et al. An anaerobic hybrid bioreactor of granular and immobilized biomass for anaerobic digestion (AD) and dark fermentation (DF) of palm oil mill effluent: mass transfer evaluation in granular sludge and role of internal packing. Biomass Bioenergy. 2017;103:1–10. doi:10.1016/j.biombioe.2017.05.006
[7] da Silva Ramos JGV, Leon FdA, Michelon LK, et al. Recovery of methane dissolved in the effluent of a novel upflow anaerobic hybrid reactor (UAHB) submitted to temperature variation. Environ Technol. 2021;0:1–33.
[8] Büyükkamaci N, Filibeli A. Concentrated wastewater treatment studies using an anaerobic hybrid reactor. Process Biochem. 2002;38(5):771–775. doi:10.1016/S0032-9592(02)00221-2
[9] Michelon L, Ramos J, Carvalho K, et al. Effects of temperature and HRT on biogas production in moving and

fixed bed of a novel Upflow Anaerobic Hybrid (UAHB) reactor. Environ Technol. 2022;44:1–37.

[10] Godinho J, Arantes E, Carvalho K, et al. Comportamento dinâmico e hidrodinâmico de reator tipo UASB submetido à variação de carga hidráulica. Revista DAE. 2017;66:84–98. doi:10.4322/dae.2017.017

[11] Banu JR, Kaliappan S. Treatment of tannery wastewater using hybrid upflow anaerobic sludge blanket reactor. J Environ Eng Sci. 2007;6(4):415–421. doi:10.1139/s06-063

[12] Das S, Chaudhari S. Effect of reactor configuration on performance during anaerobic treatment of low strength wastewater. Environ Technol. 2015;36(18):2312–2318.

[13] Loganath R, Mazumder D. Performance study on enlarged-clarifier hybrid upflow anaerobic sludge blanket reactor for treating the slaughterhouse wastewater. Water Environ J. 2020;34(S1):516–528. doi:10.1111/wej.12555

[14] Rajakumar R, Meenambal T, Saravanan PM, et al. Treatment of poultry slaughterhouse wastewater in hybrid upflow anaerobic sludge blanket reactor packed with pleated poly vinyl chloride rings. Bioresour Technol. 2012;103(1):116–122. doi:10.1016/j.biortech.2011.10.030

[15] Musa MA, Idrus S. Effect of hydraulic retention time on the treatment of real cattle slaughterhouse wastewater and biogas production from HUASB reactor. Water. 2020;12(2):490. doi:10.3390/w12020490

[16] De Mendonça HV, Ometto JPHB, Otenio MH, et al. Bioenergy recovery from cattle wastewater in an UASB-AF hybrid reactor. Water Sci Technol. 2017;76(9):2268–2279. doi:10.2166/wst.2017.325

[17] Lavanya R, Jodhi C. Evaluation studies on hybrid up flow anaerobic sludge blanket reactor for treating dairy effluent under different season. Int J Eng Res Appl. 2016;6(3):61–66.

[18] Narra M, Balasubramanian V, Mehta H, et al. Performance evaluation of anaerobic hybrid reactors with different packing media for treating wastewater of mild alkali treated rice straw in ethanol fermentation process. Bioresour Technol. 2014;152:59–65. doi:10.1016/j.biortech.2013.10.071

[19] Fia FRL, Matos AT, Borges AC, et al. Treatment of wastewater from coffee bean processing in anaerobic fixed bed reactors with different support materials: performance and kinetic modeling. J Environ Manag. 2012;108:14–21.

[20] Selvamurugan M, Doraisamy P, Maheswari M, et al. High rate anaerobic treatment of coffee processing wastewater using upflow anaerobic hybrid reactor. Iranian J Environ Health Sci Eng. 2010;7(2):129–136.

[21] Thiyagu R, Sivarajan P. Influence of organic loading rate in acclimatization phase of hybrid upflow anaerobic sludge blanket (UASB) reactor treating distillery spent wash. Nature Environ Pollut Technol. 2018;17(1):223–227.

[22] Ramdhanie I, Chakrabarti DP. Studies on the design, evaluation, and energy conservation potential of a pilot-scale hybrid uasb treating a combination of waste activated sludge and distillery spent wash. Chem Eng Commun. 2014;201(6):804–833. doi:10.1080/00986445.2013.791812

[23] Subramani T, Krishnan S, Kumaresan PK, et al. Treatability studies on hybrid up-flow anaerobic sludge blanket reactor for pulp and paper mill wastewater. Int J Mod Eng Res. 2012;2(3):602–606.

[24] Oktem YA, Ince O, Sallis P, et al. Anaerobic treatment of a chemical synthesis-based pharmaceutical wastewater in a hybrid upflow anaerobic sludge blanket reactor. Bioresour Technol. 2008;99(5):1089–1096. doi:10.1016/j.biortech.2007.02.036

[25] Priya M, Meenambal T, Balasubramanian N, et al. Comparative study of treatment of sago wastewater using HUASB reactor in the presence and absence of effective microorganisms. Procedia Earth Planet Sci. 2015;11:483–490. doi:10.1016/j.proeps.2015.06.048

[26] Yanqoritha N, Turmuzi M, Irvan I, et al. Acclimatization process on Hybrid Upflow Anaerobic Sludge Blanket Reactor (HUASBR) using bioball as growth media with OLR variation for treating tofu wastewater. Orient J Chem. 2018;34(6):3100–3105. doi:10.13005/ojc/340654

[27] Ravichandran P, Balaji K. Effect of HRT on performance of hybrid upflow anaerobic sludge blanket (HUASB) reactor using bio balls in treatment of pulp and paper mill bagasse wash water. Mater Today Proc. 2020;22(xxxx):627–632. doi:10.1016/j.matpr.2019.09.011

[28] Paixão MA, Tavares CRG, Bergamasco R, et al. Anaerobic digestion from residue of industrial cassava industrialization with acidogenic and methanogenic physical separation phases. Appl Biochem Biotechn – Part A Enzym Eng Biotechnol. 2000;84–86(1):809–819. doi:10.1385/ABAB:84-86:1-9:809

[29] Elmitwalli TA, Oahn KLT, Zeeman G, et al. Treatment of domestic sewage in a two-step anaerobic filter/anaerobic hybrid system at low temperature. Water Res. 2002;36(9):2225–2232. doi:10.1016/S0043-1354(01)00438-9

[30] Henze M, Van Loosdrecht MCM, Ekama GA, et al. Biological wastewater treatment: principles, modelling and design [Internet]. IWA Publishing; 2008 [cited 2025 Mar 17]. Available from: http://iwaponline.com/ebooks/book/59/Biological-Wastewater-Treatment-Principles.

[31] Sørensen KH, Morgenroth E. Biofilm reactors. Biological wastewater treatment [Internet]. 2023 [cited 2025 Mar 17];(2). doi:10.2166/9781789060362_0813.

[32] Latif MA, Ghufran R, Wahid ZA, et al. Integrated application of upflow anaerobic sludge blanket reactor for the treatment of wastewaters. Water Res. 2011;45(16):4683–4699. doi:10.1016/j.watres.2011.05.049

[33] Patel BB, DrPJ G, DrUD P, et al. Hydrodynamics of hybrid upflow anaerobic sludge blanket reactors using tracer studies. Environ Challenges. 2021;5:100358. doi:10.1016/j.envc.2021.100358

[34] Patel BB, Gundaliya PJ, Amin DD. Optimized hybrid upflow anaerobic sludge blanket with post treatment processes for wastewater. Current World Environment [Internet]. 2021 [cited 2025 Mar 14]; doi:10.12944/CWE.16.1.29.

[35] Reynolds O. XXIX. An experimental investigation of the circumstances which determine whether the motion of water shall be direct or sinuous, and of the law of

resistance in parallel channels. Philos Trans R S London. 1883;174:935–982. doi:10.1098/rstl.1883.0029
[36] Schmidt E. Die Grundbegriffe der Wärmeübertragung. In: Schmidt E, editor. Einführung in die Technische Thermodynamik und in die Grundlagen der chemischen Thermodynamik [Internet]. 1st ed. Berlin, Heidelberg: Springer; 1963 [cited 2025 Mar 18]. p. 347–395. doi:10.1007/978-3-662-25915-3_17.
[37] Sherwood TK, Pigford RL, Wilke CR. Mass transfer. New York: McGraw-Hill; 1975.
[38] Péclet E. Traité de la chaleur, et de ses applications aux arts et aux manufactures. 1st ed Paris: Librarie scientifique industriale; 1828.
[39] Ergun S. Fluid flow through packed columns [Internet]. SciSpace - Paper. 1952 [cited 2025 Mar 18]. p. 89–94. Available from: https://scispace.com/papers/fluid-flow-through-packed-columns-32ay002rb0.
[40] Ferro TN, de Carvalho KQ, de Lima MX, et al. Influence of HRT and carbon source on the enhancement of nutrient removal in an Anaerobic-Oxic-Anoxic (AOA) system. Environ Technol. 2022;43(16):2478–2491. doi:10.1080/09593330.2021.1882586
[41] Mannich PKA, Santos DCD, Mannich M. Sistema biológico alternativo para pós-tratamento de esgoto. RDAE. 2009;57(181):23–32. doi:10.4322/dae.2014.043
[42] Torres P, Foresti E. Domestic sewage treatment in a pilot system composed of UASB and SBR reactors. Water Sci Technol. 2001;44(4):247–253. doi:10.2166/wst.2001.0230
[43] Ripley LE, Boyle WC, Converse JC. Improved alkalimetric monitoring for anaerobic digestion of high-strength wastes. J Water Pollut Control Federation. 1986;58(5):406–411.
[44] Jenkins SR, Morgan JM, Zhang X. Measuring the usable carbonate alkalinity of operating anaerobic digesters. Res J Water Pollut Control Federation. 1991;63(1):28–34.
[45] Lipps WC, Braun-Howland EB, Baxter TE. Standard methods for the examination of water and wastewater [Internet]. APHA American Public Health Association; 2023 [cited 2024 Nov 13]. Available from: https://www.pharmabooks.com.br/livros/farmacia-e-bioquimica/metodos-analiticos/standard-methods-for-the-examination-of-water-and-wastewater-24th-edition-2023-versao-livro-impresso.
[46] DiLallo R, Albertson OE. Volatile acids by direct titration. Water Pollut Control Federation. 1961;33:356–365.
[47] Kaçan E, Kütahyalı C. Adsorption of strontium from aqueous solution using activated carbon produced from textile sewage sludges. J Anal Appl Pyrolysis. 2012;97:149–157. doi:10.1016/j.jaap.2012.06.006
[48] Shapiro SS, Wilk MB. An analysis of variance test for normality (Complete samples). Biometrika. 1965;52(3/4):591. doi:10.2307/2333709
[49] Pearson. VII. Mathematical contributions to the theory of evolution. – III. Regression, heredity, and panmixia. Philos T R Soc London A. 1896;187:253–318. doi:10.1098/rsta.1896.0007
[50] Kendall M. A new measure of rank correlation. Biometrika. 1938;30(1–2):81–93. doi:10.1093/biomet/30.1-2.81
[51] Evans JD. Straightforward statistics for the behavioral sciences. J Am Stat Assoc. 1996;91(436):1750.
[52] Wu B. Integration of mixing, heat transfer, and biochemical reaction kinetics in anaerobic methane fermentation. Biotech Bioeng. 2012;109(11):2864–2874. doi:10.1002/bit.24551
[53] Maclean DJ, Alboussière T. Measurement of solute diffusivities. Part I. Analysis of coupled solute buoyancy-driven convection and mass transport. Int J Heat Mass Transfer. 2001;44(9):1639–1648. doi:10.1016/S0017-9310(00)00308-2
[54] Huysmans M. Dassargues aLAIN. Review of the use of Péclet numbers to determine the relative importance of advection and diffusion in low permeability environments. Hydrol J. 2005;13:895–904. doi:10.1007/s10040-004-0387-4
[55] Rather MA, Gupta K, Mandal M. Microbial biofilm: formation, architecture, antibiotic resistance, and control strategies. Braz J Microbiol. 2021;52(4):1701–1718. doi:10.1007/s42770-021-00624-x
[56] Moreira JMR, Simões M, Melo LF, et al. The combined effects of shear stress and mass transfer on the balance between biofilm and suspended cell dynamics. Desalin Water Treat. 2015;53(12):3348–3354. doi:10.1080/19443994.2014.933625
[57] SIMEPAR - Boletim Climatológico [Internet]. [cited 2024 Oct 21]. Available from: https://www.simepar.br/simepar/timeline/boletim_climatologico.
[58] Metcalf E, Eddy H. Wastewater engineering: treatment and reuse. Scientific Research Publishing, editor. Wastewater Engineering, Treatment, Disposal and Reuse Techobanoglous G, Burton FL, Stensel HD (eds) Tata McGraw-Hill Publishing Company Limited, 4th edition New Delhi, India. 3rd ed. 2003;1819.
[59] Van Haandel A, Coraucci Filho B, Chernicharo CJ. Tratamento de esgotos sanitários por processo anaeróbio e disposição controlada no solo. Rio de Janeiro: Prosab; 2009.
[60] Gerardi MH. Wastewater bacteria. Pennsylvania: John Wiley & Sons; 2006.
[61] Jaimes-Estévez J, Zafra G, Martí-Herrero J, et al. Psychrophilic full scale tubular digester operating over eight years: complete performance evaluation and microbiological population. Energies. 2021;14(1):151. doi:10.3390/en14010151
[62] Daija L, Selberg A, Rikmann E, et al. The influence of lower temperature, influent fluctuations and long retention time on the performance of an upflow mode laboratory-scale septic tank. Desalin Water Treat. 2016;57(40):18679–18687. doi:10.1080/19443994.2015.1094421
[63] Hoyos N, Barroso junior JC, Leal F, et al. Proposta de nova configuração de reator anaeróbio híbrido aplicado ao tratamento de esgoto sanitário. Revista DAE. 2019;67:73–88. doi:10.4322/dae.2019.046
[64] Wang N-X, Lu X-Y, Tsang Y-F, et al. A comprehensive review of anaerobic digestion of organic solid wastes in relation to microbial community and enhancement process. J Sci Food Agric. 2019;99(2):507–516. doi:10.1002/jsfa.9315
[65] Qiu S, Zhang X, Xia W, et al. Effect of extreme pH conditions on methanogenesis: methanogen metabolism and community structure. Sci Total Environ. 2023;877:162702.
[66] Kullavanijaya P, Thongduang P, Boonapatcharoen N, et al. The methanogenic archaea characteristics and

efficacy of aerobic waste sludge in the start-up of anaerobic hybrid reactors treating cassava wastewater. Environ Eng Res. 2021;27(4):210162–0. doi:10.4491/eer.2021.162

[67] Sun M, Liu B, Yanagawa K, et al. Effects of low pH conditions on decay of methanogenic biomass. Water Res. 2020;179:115883. doi:10.1016/j.watres.2020.115883

[68] Silva Vd, Campos CMM, Pereira EL, et al. Start-up and steady-state conditions of an Anaerobic Hybrid Reactor (AHR) using mini-filters composed with two types of support medium operating under low loading rates. Braz Arch Biol Technol. 2011;54:973–982. doi:10.1590/S1516-89132011000500015

[69] Sperling Mv. Basic principles of wastewater treatment. London: IWA Publishing; 2007.

[70] Fia FRL, Borges AC, Matos Ad, et al. Development of biofilm in anaerobic reactors treating wastewater from coffee grain processing. Rev Bras Eng Agríc Amb. 2010;14:210–217. doi:10.1590/S1415-43662010000200013

[71] Pereira EL, Campos CMM, Motteran F. Physicochemical study of pH, alkalinity and total acidity in a system composed of anaerobic baffled reactor in series with Upflow Anaerobic Sludge Blanket reactor in the treatment of pig farming wastewater. Acta Scientiarum Technol. 2013;35(3):477–483.

[72] López-López A, León-Becerril E, Rosales-Contreras ME, et al. Influence of alkalinity and VFAs on the performance of an UASB reactor with recirculation for the treatment of Tequila vinasses. Environ Technol. 2015;36(19):2468–2476. doi:10.1080/09593330.2015.1034790

[73] Foresti E. Fundamentos do processo de digestão anaeróbia. In: Seminário Latino Americano. 3, Montevidéo. Anais…, Montevidéo; 1994. p. 97–110.

[74] Silva Gd, Nour EAA. Reator compartimentado anaeróbio/aeróbio: sistema de baixo custo para tratamento de esgotos de pequenas comunidades. Rev Bras de Eng Agr Amb. 2005;9(2):268–275. doi:10.1590/S1415-43662005000200019

[75] Souza Gd, Oliveira Ld, Bello IP, et al. Use of coffee capsules as support material in upflow anaerobic fixed bed reactors. Braz Arch Biol Technol. 2019;62:e19180504. doi:10.1590/1678-4324-2019180504

[76] Pérez A, Torres P. Indices de alcalinidad para el control del tratamiento anaerobio de aguas residuales fácilmente acidificables (Alkalinity indices for control of anaerobic treatment of readily acidifiable wastewaters). Ingeniería y Competitividad. 2008;10(2):41–52. doi:10.25100/iyc.v10i2.2473

[77] Santana Ad, Oliveira Rd. Desempenho de reatores anaeróbios de fluxo ascendente com manta de lodo em dois estágios tratando águas residuárias de suinocultura. Eng Agríc. 2005;25:817–830. doi:10.1590/S0100-69162005000300029

[78] Hernández DM, Hurtado LdP, Rodríguez-Chaparro AT. Hydrogen production in a novel configuration of UASB reactor under different hydraulic retention time. DYNA. 2018;85(205):157–162. doi:10.15446/dyna.v85n205.70494

[79] Lettinga G. Anaerobic digestion and wastewater treatment systems. Antonie Van Leeuwenhoek (Journal of Microbiology). 1995;67(1):3–28. doi:10.1007/BF00872193

[80] Schink B. Energetics of syntrophic cooperation in methanogenic degradation. Microbiol Mol Biol Rev. 1997;61(2):262–280.

[81] Harirchi S, Wainaina S, Sar T, et al. Microbiological insights into anaerobic digestion for biogas, hydrogen or volatile fatty acids (VFAs): a review. Bioengineered. 2022;13(3):6521–6557. doi:10.1080/21655979.2022.2035986

[82] Liang P, Yuan L, Yang X, et al. Coupling ion-exchangers with inexpensive activated carbon fiber electrodes to enhance the performance of capacitive deionization cells for domestic wastewater desalination. Water Res. 2013;47(7):2523–2530. doi:10.1016/j.watres.2013.02.037

[83] Silley P, Forsythe S. Impedance microbiology – a rapid change for microbiologists. J Appl Bacteriol. 1996;80(3):233–243. doi:10.1111/j.1365-2672.1996.tb03215.x

[84] Tortorello ML, Gendel SM. Food microbiology and analytical methods. 1st ed. 1997; p. 321–330. doi:10.1201/9781482269833

[85] Hawkes FR, Guwy AJ, Hawkes DL, et al. On-line monitoring of anaerobic digestion: application of a device for continuous measurement of bicarbonate alkalinity. Water Sci Technol. 1994;30(12):1–10. doi:10.2166/wst.1994.0571

[86] Loganath R, Mazumder D. Performance study on organic carbon, total nitrogen, suspended solids removal and biogas production in hybrid UASB reactor treating real slaughterhouse wastewater. J Environ Chem Eng. 2018;6(2):3474–3484. doi:10.1016/j.jece.2018.05.031

[87] Hemalatha D, Keerthinarayana S. Kinetic modelling of hybrid upflow anaerobic sludge blanket reactor in treatment of pulp and paper mill wastewater. Indian J Chem Technol. 2017;24(3):352–357.

[88] Balasundaram N, Meenambal T, Balasubramanium N, et al. Comparative study of different media in the treatment of sago wastewater using HUASB reactor. Nature Environ Pollut Technol. 2014;13(3):511–516.

[89] Matsunaga K, Kindaichi T, Ozaki N, et al. Development of anammox reactor equipped with a degassing membrane to improve biomass retention. Water Sci Technol. 2012;66(2):451–456. doi:10.2166/wst.2012.222

[90] Björnsson L, Murto M, Jantsch TG, et al. Evaluation of new methods for the monitoring of alkalinity, dissolved hydrogen and the microbial community in anaerobic digestion. Water Res. 2001;35(12):2833–2840. doi:10.1016/S0043-1354(00)00585-6

[91] Enitan AM, Adeyemo J, Swalaha FM, et al. Anaerobic digestion model to enhance treatment of brewery wastewater for biogas production using UASB reactor. Environ Model Assess. 2015;20(6):673–685. doi:10.1007/s10666-015-9457-3

[92] Lew B, Tarre S, Belavski M, et al. UASB reactor for domestic wastewater treatment at low temperatures: A comparison between a classical UASB and hybrid UASB-filter reactor. Water Sci Technol. 2004;49(11–12):295–301. doi:10.2166/wst.2004.0865

[93] Gundkal Prajwal S, Bagawan Samreen A, Hogarti Manjunath J, et al. Treatment of dairy industry wastewater by hybrid upflow anaerobic sudge blanket reactor. Int J Eng Res Technol. 2019;6(9):1257–1263.

[94] Ayati B, Ganjidoust H. Comparing the efficiency of UAFF and UASB with hybrid reactor in treating wood

fiber wastewater. J Environ Health Sci Eng. 2006;3(1): 39–44.

[95] Sreekanth D, Sivaramakrishna D, Himabindu V, et al. Thermophilic treatment of bulk drug pharmaceutical industrial wastewaters by using hybrid up flow anaerobic sludge blanket reactor. Bioresour Technol. 2009;100(9):2534–2539. doi:10.1016/j.biortech.2008.11.028

[96] Trivedi RD, Vyas DS, Patel SM. Hybrid UASB reactor: a research evaluation for treatment of pharmaceutical industry wastewater. Int J Current Microbiol Appl Sci. 2019;8(04):1453–1461. doi:10.20546/ijcmas.2019.804.170

[97] Murugesan EMP, Selvarasu P. Experimental investigation of HUASB reactor for treatment characteristics of leather effluent with varying of different operating parameters. Int J Chem Tech Res. 2017;10(6):478–484.

[98] Chaiprasert P, Suvajittanont W, Suraraksa B, et al. Nylon fibers as supporting media in anaerobic hybrid reactors: it's effects on system's performance and microbial distribution. Water Res. 2003;37(19):4605–4612. doi:10.1016/S0043-1354(03)00422-6

[99] Rajesh Banu J, Kaliappan S, Beck D. High rate anaerobic treatment of sago wastewater using HUASB with PUF as carrier. Int J Environ Sci Technol. 2006;3(1):69–77. doi:10.1007/BF03325909

[100] Zhang Y, Ma Y, Quan X, et al. Rapid startup of a hybrid UASB-AFF reactor using bi-circulation. Chem Eng J. 2009;155(1–2):266–271. doi:10.1016/j.cej.2009.08.005

[101] Yanqoritha N, Turmuzi M, Irvan I, et al. The effect of organic loading rate variation on digestion of tofu wastewater using PVC rings as growth media in a hybrid UASB reactor. Orient J Chem. 2018;34(3):1653–1657. doi:10.13005/ojc/340361

[102] Gupta SK, Gupta SK, Singh G. Anaerobic hybrid reactor: A promising technology for treatment of distillery spent wash. Int J Environ Pollut. 2010;43(1–3):221–235. doi:10.1504/IJEP.2010.035926

[103] Rajagopal R, Mehrotra I, Kumar P, et al. Evaluation of a hybrid upflow anaerobic sludge-filter bed reactor: effect of the proportion of packing medium on performance. Water Sci Technol. 2010;61(6):1441–1450. doi:10.2166/wst.2010.081